表8　ウイルス初感染・再感染・再活性化と抗体パターン

感染様式	IgM 抗体	IgG 抗体	
		抗体価	avidity
初感染	＋～＋＋	－～＋	弱い
再感染	－～＋	＋＋＋	強い
ワクチン後感染			
一次性ワクチン不全	＋～＋＋	－～＋	弱い
二次性ワクチン不全	－～＋	＋＋＋	強い
再活性化	－～＋	＋＋＋	強い

・ウイルス再感染，二次性ワクチン不全，再活性化時には，IgG 抗体は発症早期から上昇していることがあり，有意上昇を示さないことがある．
・avidity とは抗原と抗体の結合力のことであり，IgG3 画分に属する抗体は結合力が弱く，IgG1 画分に属する抗体は結合力が強い．再感染などでは早期から IgG1 画分の抗体が上昇するため急性期の血清でも強い avidity が認められる．

量に応じた免疫反応であり，時間の経過とともに IgG 抗体も IgM 抗体も上昇する．1 回の血清 IgM 抗体検査で感染症を診断するためには，発症 48 時間以降に測定することが望まれている．非特異陽性の場合は，時間の経過による IgM 抗体の上昇が認められない．

血清抗体の有意上昇とは，急性期と回復期（急性期から原則 2 週間以上あける）の血清抗体価が測定誤差以上に上昇することである．抗体価が倍で表される方法では 2 管（4 倍）以上の，抗体価が単位で表される方法では 2 倍以上の上昇である．

ウイルス感染症再感染，二次性ワクチン不全によるウイルス感染の場合は，ときに発症前から二次免疫応答が始まるため，急性期の血清抗体パターンは，IgM 抗体陰性または弱陽性，IgG 抗体高値を示す（表 8）．IgG 抗体は早期から上昇しているため，有意上昇を示さないことがある．ウイルス再活性化時の抗体パターンは再感染時と同様である．

初感染と再感染の血清診断に，抗原と抗体との結合力（avidity）を測定する方法がウイルスやトキソプラズマなどで用いられている[16]．初感染の場合，まず循環性 B 細胞依存性形質細胞が抗原との結合力が弱い IgG3 画分に属する抗体を産生し，その後，濾胞性 B 細胞依存性形質細胞が抗原との結合力が強い IgG1 画分の抗体を産生する．一方，再感染や二次性ワクチン不全の場合は，循環性 B 細胞依存性形質細胞も抗体を産生するが，早期から濾胞性 B 細胞依存性形質細胞が抗体を産生するため，発症早期でも avidity の強い抗体が検出される．抗体の avidity 測定は，8 モル尿素を含む洗浄液による EIA にて測定する．Avidity が弱い抗体では尿素を含む洗浄液で洗浄すると抗体価が著明に低下する．

2）免疫状態の診断

個人の免疫状態を調べるための代表的な抗体測定方法を表 7 に示した．麻疹発症を予防する抗体価は 120mIU/mL であり，この抗体価は NT では 4 倍，EIA では 4.0EIA 価，PA では 64 倍に相当する[17]．また，風疹発症を予防する抗体価は 4～10IU/mL であり，10IU/mL とすると，HI 抗体では 16 倍，EIA では 5.0EIA 価に相当する．ワクチン後の免疫を調べるときは，感度，特異度ともに優れた方法で測定する必要がある．

■先天性ウイルス感染症の診断

ウイルス感染症の特別な型として先天性ウイルス感染症がある．先天性ウイルス感染症の診断方法を表 9 に示した[18]．特徴的な症状として，低出生体重児，肝脾腫，出血斑，脳内石灰化，白内障・網膜症，難聴などがある．ウイルスが児に先天性感染すると多くは持続感染するため，胎内の感染

表9　先天性ウイルス感染症の診断

①特徴的な臨床症状
②出生時のIgM抗体≧20mg/dL
③ウイルス分離（原則生後3週以内）
　・尿，唾液，眼房水（先天性風疹症候群）
④ウイルス核酸の検出（PCR, real-time PCR, LAMP）
　・臍帯，尿，唾液
⑤特異的IgM抗体の検出

・IgG抗体は母体からの移行があるため早期診断に用いにくい．
・CMVは周産期感染，母乳感染があるため先天性感染の診断は生後3週間以内に診断するか，3週間以上経過した場合は乾燥臍帯を用いて診断する．
・主として母乳により感染するヒトT細胞白血病ウイルス(HTLV-1)感染の診断は3歳時に行う．

時期にかかわらず出生時からIgM抗体は検出される．IgG抗体は母体から児に移行するため，早期診断には用いられない．

おわりに

ウイルス感染症の診断方法について解説した．適切にサンプルを採取し，適切にサンプルを輸送し，適切に診断方法を使い分け，適切に診断することが大切である．

文　献

1) 庵原俊昭：ウイルス感染症の診断．小児科診療 68：1992-1999, 2005.
2) 庵原俊昭：麻疹・風疹・水痘・ムンプスに対する病院および地域における感染制御対策の最近の動向．医療 60：483-488, 2006.
3) 庵原俊昭：麻疹・風疹・ムンプス（流行性耳下腺炎）・水痘感染対策：抗体測定とその評価．CAMPUS HEALTH 45：9-14, 2008.
4) 庵原俊昭：抗体検査：目的・結果・次にすることは．小児感染免疫 23：89-95, 2011.
5) 庵原俊昭：ムンプスワクチン接種後のムンプス罹患時における病態と臨床像の特徴．小児科 42：1144-1149, 2001.
6) 庵原俊昭，豊田美香，中野貴司ほか：アメリカ微生物学会（ASM）のウイルス分離用採取ガイドラインからみたわが国のコマーシャルラボの採取方法の検討．小児感染免疫 11：103-107, 1999.
7) 川上千春，渡邉寿美，清水英明ほか：インフルエンザウイルス．臨床とウイルス 40：104-112, 2012.
8) 藤本嗣人，花岡　希，小長谷昌未ほか：アデノウイルス．臨床とウイルス 40：115-122, 2012.
9) 高尾信一：RSウイルス，ヒト・メタニューモウイルス．臨床とウイルス 40：124-133, 2012.
10) 水田克己：エンテロウイルス・ライノウイルス．臨床とウイルス 40：134-141, 2012.
11) 改田　厚，久保英幸，入谷典弘ほか：ヒトパラインフルエンザウイルス感染症．臨床とウイルス 40：142-149, 2012.
12) 庵原俊昭：ウイルス検査法とその評価－抗体測定方法を中心に－．第11回SRL感染症フォーラム講演集：4-15, 2007.
13) 田中敏博，小栗　泉，川出博江：伝染性紅斑の成人患者における血清中の麻疹ウイルスIgM抗体価の変動．病原微生物検出情報 31：268-269, 2010.
14) 佐藤　弘，多屋馨子，高崎智彦ほか：デング熱および突発性発疹と考えられる症例における麻疹IgM抗体陽性例．病原微生物検出情報 31：269-271, 2010.
15) 庵原俊昭，中野貴司，落合　仁ほか：改良されたムンプス酵素免疫法(EIA)-IgM抗体検査法の臨床評価．小児感染免疫 23：123-129, 2011.
16) 庵原俊昭，谷口清州，神谷　齊ほか：ワクチン後のムンプス罹患例におけるムンプスIgG抗体とそのAvidityの検討．臨床とウイルス 24：389-393, 1996.
17) 庵原俊昭ほか：風疹・麻疹抗体測定法の標準化に関する研究：抗体測定方法の互換性と感染予防レベルの検討．ウイルス感染症の体外診断薬の再評価に関する基盤整備に関する研究（研究代表者：小林和夫）平成21年度総括・分担研究報告書, pp19-25, 2010.
18) 堤　裕幸：健常児におけるウイルス感染症．小児感染免疫 23：403-407, 2012.

＊　　＊　　＊

Graefes Arch Clin Exp Ophthalmol (2010) 248:1487–1491
DOI 10.1007/s00417-010-1434-6

INFLAMMATORY DISORDERS

Rubella virus as a possible etiological agent of Fuchs heterochromic iridocyclitis

Jun Suzuki · Hiroshi Goto · Katsuhiro Komase · Hitoshi Abo · Kaoru Fujii · Noriyuki Otsuki · Kiyoko Okamoto

Received: 2 February 2010 / Revised: 10 May 2010 / Accepted: 12 June 2010 / Published online: 29 June 2010

Abstract
Background To determine whether rubella virus is involved in the pathogenesis of Fuchs heterochromic iridocyclitis (FHI).
Methods Fourteen patients (14 eyes) diagnosed with FHI based on characteristic ocular manifestations and eight control subjects were studied. Aqueous humor (AH) samples from 14 FHI patients and one vitreous sample from a FHI patient were analyzed for intraocular antibody production against rubella virus by calculation of the Goldmann–Witmer coefficient (GWC). Viral detection by nested polymerase chain reaction and isolation by culture in RK-13 cells were conducted in nine FHI patients. In addition to laboratory examinations, medical history of rubella virus vaccination was also obtained.
Results Ten patients with FHI examined showed intraocular synthesis of rubella virus antibodies (GWC>3). A high index of rubella virus antibody production was also found in the vitreous sample (GWC=30.6). GWC in all control subjects were below detectable level. The rubella genome was detected in two of nine patients, and rubella virus was isolated from one of nine patients with FHI. None of the patients with FHI had been vaccinated against rubella.
Conclusions Our laboratory data strongly suggest a relationship between FHI and rubella virus.

Keywords Fuchs heterochromic iridocyclitis · Rubella virus · Viral isolation · Vaccination

J. Suzuki (✉) · H. Goto
Department of Ophthalmology,
Tokyo Medical University Hospital,
6-7-1 Nishishinjuku, Shinjuku-ku,
Tokyo 160-0023, Japan
e-mail: jun-s@qc4.so-net.ne.jp

K. Komase · H. Abo · K. Fujii · N. Otsuki · K. Okamoto
Department of Virology III,
National Institute of Infectious Disease,
4-7-1 Gakuen, Musashi Murayama-shi,
Tokyo 208-0011, Japan

Introduction

Fuchs heterochromic iridocyclitis (FHI) is an intraocular inflammatory disease that constitutes approximately 0.5% to 6.2% of all cases of uveitis [1, 2]. FHI usually occurs in only one eye. Common clinical manifestations are: (1) chronic low-grade iridocyclitis including keratic precipitates, (2) iris heterochromia, atrophy or both, (3) absence of synechiae, and (4) early cataract [3, 4]. Complications such as glaucoma and vitreous opacities have been reported in 14.8% of patients with FHI [5]. Patients may remain asymptomatic for years, and diagnosis is often made by a decrease in visual acuity secondary to cataract which was observed in 77.8% at presentation. Therefore, it is difficult to detect FHI at the early stage and to prevent disease progression.

The etiology of FHI remains unknown. Because of the association between FHI and Horner's syndrome, sympathetic nerve dysfunction was considered to be a cause of FHI [6]. Saari et al. [7] also reported vascular abnormality of the iris in patients with FHI, as demonstrated by fluorescein angiography. In addition to the organic abnormalities in patients, some infectious agents such as *Toxoplasma gondii* [8], herpes simplex virus (HSV) [9] and cytomegalovirus (CMV) [10], as well as auto-antigens [11, 12] have been proposed as possible causes of FHI. Recently, several studies have implicated rubella virus infection as a possible etiological agent of FHI [13–16].

Table 1 Demographic and clinical background of 14 patients studied

Case	Age	Gender	Medical history	
			Rubella infection	Rubella vaccination
1	55	male	+	–
2	50	female	+	–
3	47	female	–	–
4	60	male	+	–
5	41	male	+	–
6	50	male	+	–
7	39	male	+	–
8	26	female	–	not known
9	36	female	+	–
10	27	male	+	–
11	51	male	not known	–
12	62	female	+	–
13	39	female	+	–
14	54	female	+	–

However, it is suggested that intraocular presence of rubella virus is not necessary for the development of FHI [13, 16].

The objectives of the present study were to verify the relationship between rubella virus infection and FHI by examining intraocular antibody production and detecting viral RNA by polymerase chain reaction (PCR), and to attempt to isolate rubella virus from aqueous humor of FHI patients to confirm the intraocular presence of the virus.

Material and methods

Fourteen Japanese patients (14 eyes) with FHI who attended the uveitis clinic of Tokyo Medical University Hospital between 2006 and 2009 were enrolled in this retrospective review. The study was approved by the institutional review board.

Diagnosis of FHI was based on characteristic ocular manifestations including chronic anterior intraocular inflammation, keratic precipitate, absence of posterior synechiae, heterochromia or anterior stromal iris atrophy, and secondary cataract. The demographics and clinical background of the patients with FHI are shown in Table 1.

As controls, eight Japanese patients with other types of uveitis comprising sarcoidosis (one), Posner–Schlossman syndrome (one), herpetic iritis (one), Behçet disease (one) and unclassified intraocular inflammation (four) were selected. The diseases of the control patients were clearly differentiated from FHI by clinical manifestations and laboratory studies. Demographics of FHI patients and controls are listed in Table 2.

Aqueous humor (AH) samples were obtained from all FHI patients during surgery for secondary cataract or secondary glaucoma. All patients with FHI had no or low-grade ocular inflammatory activity at the time of sample collection. One vitreous humor (VH) sample was also obtained during vitrectomy for vitreous opacity. Rubella antibody titers in intraocular fluid (AH and VH) and serum samples from 14 FHI patients were determined by fluorescent antibody (FA) and enzyme immunoassay (EIA) techniques. Paired intraocular fluid and serum samples from each patient were tested at the same time. The Goldmann–Witmer coefficient (GWC) was calculated as follows: quantity of rubella virus-specific IgG/total IgG in intraocular fluid divided by rubella virus-specific IgG/total IgG in serum. A GWC value exceeding 3 was considered to indicate local antibody production, as described previously [14].

Rubella virus detection and isolation were conducted using AH samples from the nine most recent FHI patients (cases 6 to 14). For rubella virus isolation, RK-13 cells were inoculated with AH and incubated, and the cell cultures were serially passaged. The RK-13 cells were lysed by rapid freezing and thawing, and the lysate obtained was used for reverse transcription-polymerase chain reaction (RT-PCR). For rubella virus detection from ocular samples, total RNA was extracted from the samples using the High Pure Viral RNA kit (Roche Diagnostics, UK). For detecting rubella viral RNA, two nested RT-PCR were conducted for two parts of the E1 gene, designated as E1-2 region (466 bp) and E1-3 region (423 bp). The primer designs used for RT-PCR were listed in Table 3. The first round RT-PCR was performed as follows: 50°C for 30 min, followed by 95°C for 5 min, then 40 cycles of 90°C for 30 s, 61°C for 30 sand 72°C for 1 min., and 72°C for 5 min. For the nested PCR, 25 cycles of 98°C for 10 s, 59°C for 30 s (E1-2 region) or 66°C for 30 s (E1-3 region) and 72°C for 45 s

Table 2 Demographics and clinical characteristics of FHI and control patients

RV: rubella virus, [a]: Goldmann–Witmer coefficient could not be calculated in four cases due to insufficient ocular sample for IgG measurement

*: $p<0.01$: Fisher's exact test

	FHI	Control
Cases	14	8
Male	7 (50%)	3 (38%)
Female	7 (50%)	5 (62 %)
Age (years)	45.5 (27–62)	69.5 (45–85)
Intraocular antibody production against RV	10/10[a] (100%)	0/8 (0%)*

Table 3 Primers for rubella virus RT-PCR

Region	PCR	Primer	Sequence
E1-2	First	E1-2F	5′- AGCGACGCGGCCTGCTGGG
		E1-2R	5′- CCAGCGCGTATGTGG AGTCC
	Nested	E1-6F	5′- ACACCGTGATGAGCGTGTTC
		E1-10R	5′- ATGT GGAGTCCGCACTTGCG
E1-3	First	E1-7F	5′- TTGTGGGGGCCACGCCAGAG
		E1-12R	5′- TGTGTGCCATACACCA CGCC
	Nested	E1-3F	5′- CGGCGAGGTGTGGGTCACGC
		E1-3R	5′- ACCCGCGCGCTCGCGCGATC

were conducted. The PCR products were confirmed by electrophoresis in 1.5% agarose gel.

In addition to laboratory examinations, medical history related to exposure to rubella (vaccination or infection) was also obtained.

Results

Antibody titer and GWC for rubella virus

We attempted to measure rubella antibody titers and determine GWC using paired AH and serum samples collected from 14 patients with clinically definite FHI. Ten FHI patients demonstrated intraocular synthesis of rubella virus antibodies (GWC>3) with median GWC of 45.1 (total range 5.7–186.1) (Fig. 1). In the remaining four patients with FHI (cases 11 to 14), total IgG in AH could not be measured because of inadequate AH samples, and therefore GWC could not be determined, although rubella antibody was positive in their AH samples (case 11: 32.5 IU, case 12: 130 IU, case 13: 20 IU, case 14: 28.5 IU). None of the control subjects had antibodies against rubella in AH samples and GWC values were below detectable level. The rates of intraocular antibody synthesis were significantly different ($P<0.01$; Fisher's exact test) between patients with FHI (ten of ten) and control patients (none of eight) (Table 2).

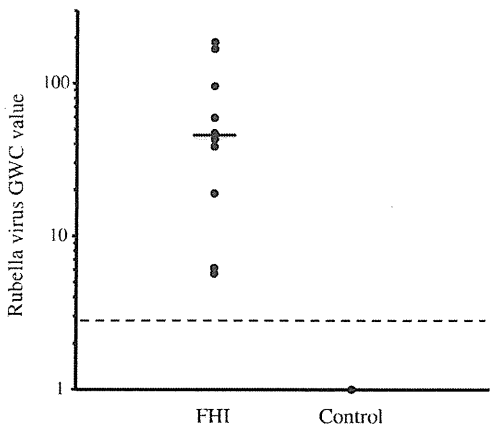

Fig. 1 Evaluation of the rubella virus Goldmann–Witmer coefficient (GWC) values of ten patients with FHI and eight control patients. The median value of FHI patients is indicated by a *horizontal black line*. The threshold GWC value 3 is indicated by the *dashed line*. The GWC value is presented in a logarithmic scale

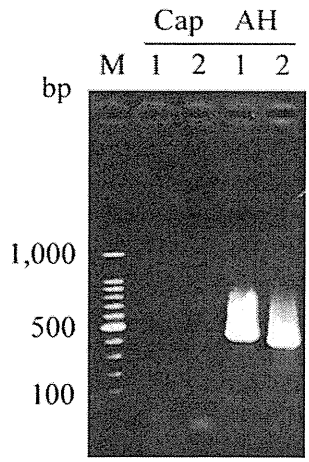

Fig. 2 Representative results of the detection of rubella virus gene from ocular samples of case 6 using two nested RT-PCR. Lanes *1 and 2* indicate the PCR products of E1-2 and E1-3 regions, respectively. Lane *M* shows the 100 bp DNA ladder markers. *Cap*; lens anterior capsule, *AH*; aqueous humor. Note that the PCR products from AH are positive for rubella virus

The vitreous sample from one FHI patient (case 6) was also examined. The rubella antibody titer in the VH sample was ×160, and total IgG was 14.9 mg/dl. The GWC of VH was high (GWC=30.6).

Rubella virus gene detection from AH and lens anterior capsule

Using RT-PCR, the rubella genome was detected in two of nine AH samples from FHI patients (cases 6 and 7). Virus detection was confirmed by two primer sets targeting the

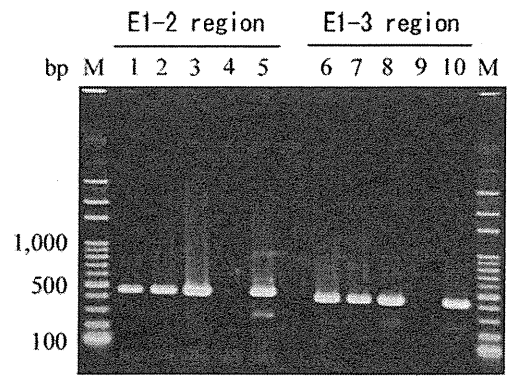

Fig. 3 Detection of rubella virus gene using RT-PCR from different passages of RK-13 cells inoculated with aqueous humor sample collected from case 7. Lanes 1-5 show the PCR results of E1-2 region, and lanes 6-10 show the PCR results of E1-3 region. Lanes 1-3 and 6-8 are the results from passages 1 to 3, respectively, of RK-13 cells inoculated with AH. Lanes 4 and 9 indicate negative control and lanes 5 and 10 indicate positive control. Lane Ms are 100 bp DNA ladder markers. Note that the PCR products from the 3rd passages of RK-13 cell are positive for rubella virus

E1 gene of rubella virus. The representative data of RT-PCR are shown in Fig. 2.

Rubella virus isolation from AH

Rubella virus isolation was attempted in nine patients with FHI (Cases 6 to 14). Rubella virus was isolated from one patient with FHI (case 7). The results of RT-PCR obtained from lysates of various passages of RK-13 cells are shown in Fig. 3.

Medical history of rubella vaccination and infection

Fourteen patients with FHI were questioned for a medical history of rubella vaccination and infection (Table 1). None of the patients with FHI had been vaccinated against rubella, although one patient was uncertain. A previous medical history of rubella infection was confirmed in 11 cases.

Discussion

Many previous reports have speculated the etiology of FHI, but recent reports of the relationship between rubella virus and FHI have renewed the interest. Quentin et al. [13] demonstrated the existence of rubella virus in AH by GWC determination and PCR assay, and de Groot-Mijnes et al. [14] confirmed the presence of rubella infection by calculating GWC. In this study, we also demonstrated rubella infection in AH and VH by GWC determination and PCR assay. The epidemiologic observation revealed reduced incidence of FHI following the introduction of vaccination against rubella virus [15]. None of our patients with FHI had received vaccination against rubella virus. Together with previous reports, these results confirmed the relationship between FHI and rubella virus.

With regard to the diagnosis of FHI, Ruokonen et al. [16] reported the usefulness of determining intraocular antibody production rather than detecting the virus gene by RT-PCR. In their report, intraocular antibody production against rubella virus was found in all cases, whereas only two of 20 cases had positive results for PCR. In our study, the rate of rubella antibody proportion was 10/10 and that of virus gene detection by PCR was 2/9, and these findings agree with Ruokonen's report.

On the other hand, rubella virus was isolated from the AH of one FHI patient in this study. Except with the congenital rubella syndrome, rubella virus is transmitted by the respiratory route, and replicates in the nasopharynx and lymph nodes and then spreads throughout the body causing fever and rash [17]. The general perception is that there is no carrier state and the reservoir exists only in active human cases. Therefore, it is unclear whether the virus detected and isolated from aqueous humor in the FHI patient was from acute infection, re-infection or re-activation of latent virus. In the case of congenital rubella syndrome, rubella virus may persist in the lens for many years [18]. We also tried to detect rubella virus from the lens anterior capsule in case 6 using RT-PCR, but the result was negative.

Since rubella virus has not been hitherto isolated from intraocular fluid of FHI patients, the genetic characters of rubella virus associated with FHI are unknown. In Japan, no nationwide epidemics of rubella have been documented since 1992 [19], but small outbreaks in local areas have been observed, and the virus genotypes isolated in various outbreaks were different [20]. By studying the genealogical background of rubella virus strains isolated from patients with FHI, it may be possible to determine the time of infection and the strain(s) with a predilection to induce FHI. Moreover, antigen-specific immune reaction has been suspected to play a role in the pathogenesis of FHI, based on the results of restriction of infiltrated T cells [21] and polymorphisms of cytotoxic T cell antigen 4 [22]. Analysis of the specific genetic modification of the rubella virus may clarify the characteristics and the tropisms of the virus. Efforts to isolate and characterize the virus from intraocular sites will elucidate the pathomechanism of FHI. Further investigations are warranted.

In summary, isolation of rubella virus from intraocular specimens of FHI patients is difficult. To the best of our knowledge, this is the first report of isolation of rubella virus from the aqueous humor of a patient with FHI. Intraocular existence of rubella virus in an FHI patient is a very interesting finding when considering the mechanism of FHI development. Although the number of samples examined in this study was small, the results confirm a relationship between rubella virus and FHI. Further investigations, especially in the isolation and characterization of rubella virus strains associated with FHI, are warranted.

References

1. Goto H, Mochizuki M, Yamaki K, Kotake S, Usui M, Ohno S (2007) Epidemiological survey of intraocular inflammation in Japan. Jpn J Ophthalmol 51:41–44
2. Tran VT, Auer C, Guex-Crosier Y, Pittet N, Herbort CP (1994) Epidemiological characteristics of uveitis in Switzerland. Int Ophthalmol 18:293–298
3. Franceschetti A (1955) Heterochromic cyclitis; Fuchs' syndrome. Am J Ophthalmol 39:50–58
4. Mohamed Q, Zamir E (2005) Update on Fuchs' uveitis syndrome. Curr Opin Ophthalmol 16:356–363
5. Velilla S, Dios E, Herreras JM, Calonge M (2001) Fuchs' heterochromic iridocyclitis: a review of 26 cases. Ocul Immunol Inflamm 9:169–175
6. Regenbogen LS, Naveh-Floman N (1987) Glaucoma in Fuchs' heterochromic cyclitis associated with congenital Horner's syndrome. Br J Ophthalmol 71:844–849

7. Saari M, Vuorre I, Nieminen H (1978) Fuchs's heterochromic cyclitis: a simultaneous bilateral fluorescein angiographic study of the iris. Br J Ophthalmol 62:715–721
8. Toledo de Abreu M, Belfort R Jr, Hirata PS (1982) Fuchs' heterochromic cyclitis and ocular toxoplasmosis. Am J Ophthalmol 93:739–744
9. Barequet IS, Li Q, Wang Y, O'Brien TP, Hooks JJ, Stark WJ (2000) Herpes simplex virus DNA identification from aqueous fluid in Fuchs heterochromic iridocyclitis. Am J Ophthalmol 129:672–673
10. Chee SP, Jap A (2008) Presumed Fuchs heterochromic iridocyclitis and Posner–Schlossman syndrome: comparison of cytomegalovirus-positive and negative eyes. Am J Ophthalmol 146:883–889
11. Hammer H, Olah M (1975) Hypersensitivity towards alpha-crystalline in the heterochromia syndrome. Albrecht Von Graefes Arch Klin Exp Ophthalmol 197:61–66
12. van der Gaag R, Broersma L, Rothova A, Baarsma S, Kijlstra A (1989) Immunity to a corneal antigen in Fuchs' heterochromic cyclitis patients. Invest Ophthalmol Vis Sci 30:443–448
13. Quentin CD, Reiber H (2004) Fuchs heterochromic cyclitis: rubella virus antibodies and genome in aqueous humor. Am J Ophthalmol 138:46–54
14. de Groot-Mijnes JD, de Visser L, Rothova A, Schuller M, van Loon AM, Weersink AJ (2006) Rubella virus is associated with Fuchs heterochromic iridocyclitis. Am J Ophthalmol 141:212–214
15. Birnbaum AD, Tessler HH, Schultz KL, Farber MD, Gao W, Lin P, Oh F, Goldstein DA (2007) Epidemiologic relationship between Fuchs heterochromic iridocyclitis and the United States rubella vaccination program. Am J Ophthalmol 144:424–428
16. Ruokonen PC, Metzner S, Ucer A, Torun N, Hofmann J, Pleyer U (2010) Intraocular antibody synthesis against rubella virus and other microorganisms in Fuchs' heterochromic cyclitis. Graefes Arch Clin Exp Ophthalmol 248:565–571
17. Kimberlin DW (2002) Rubella virus. In: Richman DD, Whitley RJ, Hayden FG (eds) Clinical virology. ASM Press, Washington, DC, pp 1211–1225
18. Mets MB, Chhabra MS (2008) Eye manifestations of intrauterine infections and their impact on childhood blindness. Surv Ophthalmol 53:95–111
19. Katow S (2004) Surveillance of congenital rubella syndrome in Japan, 1978-2002: effect of revision of the immunization law. Vaccine 22:4048–4091
20. Nakayama T (2009) Laboratory diagnosis of measles and rubella infection. Vaccine 27:3228–3229
21. Labalette P, Caillau D, Grutzmacher C, Dessaint JP, Labalette M (2002) Highly focused clonal composition of CD8(+) CD28(neg) T cells in aqueous humor of fuchs heterochromic cyclitis. Exp Eye Res 75:317–325
22. Spriewald BM, Lefter C, Huber I, Lauer B, Wenkel H (2007) A suggestive association of fuchs heterochromic cyclitis with cytotoxic T cell antigen 4 gene polymorphism. Ophthalmic Res 39:116–120

Journal of Virological Methods 168 (2010) 267–271

Contents lists available at ScienceDirect

Journal of Virological Methods

journal homepage: www.elsevier.com/locate/jviromet

Short communication

Development of a novel TaqMan real-time PCR assay for detecting rubella virus RNA

Kiyoko Okamoto*, Kaoru Fujii, Katsuhiro Komase

Laboratory of Rubella, Department of Virology III, National Institute of Infectious Diseases, Murayama Branch 4-7-1 Gakuen, Musashimurayama, Tokyo 208-0011, Japan

Article history:
Received 8 January 2010
Received in revised form 18 May 2010
Accepted 25 May 2010
Available online 1 June 2010

Keywords:
Rubella
Diagnosis
TaqMan
RT-PCR

A B S T R A C T

Although the number of cases of rubella and congenital rubella syndrome has decreased recently in Japan, both are still important health problems. To control rubella infection, a rapid and reliable method for diagnosis of rubella is required as soon as possible. Direct detection of the viral genome in clinical samples is viewed as crucial for laboratory diagnosis. In this study, a novel diagnostic method for rubella virus, based on a fluorogenic real-time PCR (TaqMan) assay, was developed, and its sensitivity for various virus strains was compared with that of a conventional RT-PCR. The new assay allowed more rapid and sensitive detection of the virus than did the conventional RT-PCR, and could detect at least 10 pfu of the native strains in Japan (1a, 1D, 1j).

Rubella is caused by infection with *Rubella virus* (RV), and the symptoms include a mild rash and a fever. The most severe effect of RV infection is the congenital rubella syndrome (CRS), which is caused by infection during early pregnancy and may result in abortion, miscarriage, stillbirth, and severe birth defects. The most common congenital defects are sensorineural deafness, heart disease, and cataracts. RV belongs to the genus *Rubivirus*, family *Togaviridae*, and possesses a positive-sense, single-stranded RNA with a 9.8-kb nucleotide length that contains two open reading frames (ORFs). The 5′- and 3′-ORFs encode the nonstructural proteins p150 and p90 (Liang and Gillam, 2000; Pugachev et al., 1997) and the structural protein capsid, E1 and E2, respectively (Frey, 1994; Oker-Blom et al., 1984; Yao et al., 1998).

In Japan, single-dose rubella vaccination was started in 1976, and two-dose vaccination against measles and rubella by a combined Measles and Rubella (MR) vaccine was introduced in 2006. In 2008, a national vaccination campaign to control measles and rubella was introduced, with the aim of eliminating measles and decreasing rubella by the year 2012. To support this effectively, an active surveillance system including a rapid and reliable method for laboratory confirmation is essential. Current laboratory diagnosis employs mainly serological methods that measure anti-rubella IgM, although it takes at least 5 days after the onset of infection to detect a specific increase in anti-rubella IgM. Detection of viral RNA, for example, in oral fluid, is possible by RT-PCR if samples are obtained during the first 4–5 days after the onset of a rash (CDC, 2008). Rubella symptoms are similar to those of other viral infections (e.g. measles virus, echovirus, or parvovirus B19), making it difficult to differentiate rubella from other viral infections on the basis of clinical symptoms alone (WHO, 2007a). Other viruses such as measles and parvovirus B19 sometimes give rise to false-positive IgM results (Tipples et al., 2004).

Therefore, detection of the RV genome is considered to be a promising approach for monitoring rubella because of its sensitivity and specificity. Although several RT-PCR assays for the detection of the RV genome in clinical specimens have been described (Cooray et al., 2006; Jin and Thomas, 2007; Vyse and Jin, 2002; Zhu et al., 2007), the conventional methods require a long time and multiple procedures, and are susceptible to carry-over contamination when multiple samples, including positive samples, are tested. Real-time PCR does not require post-PCR sample handling and seems to be more feasible for much faster and higher-throughput assays. Although some investigators have described real-time PCR methods for detecting the RV genome (Abernathy et al., 2009; Hübschen et al., 2008; Rajasundari et al., 2008; Zhao et al., 2006), there has been no report confirming the sensitivity and specificity between various viral strains, or excluding the possibility of false-positive results for other viruses exhibiting similar symptoms. In this study, a novel real-time PCR system that included one-step RT-PCR for the diagnosis of rubella infection was developed and the sensitivity was compared with that of a conventional nested RT-PCR, which covers the sequencing region for genotyping, using synthesized RNA and various virus strains. This system permits detection of a minimum of 10 copies of a positive control RNA and 1 pfu of RV.

Twenty-six complete sequences of RV accessible on GenBank were aligned, and a highly conserved region was selected in design-

* Corresponding author. Tel.: +81 42 561 0771; fax: +81 42 561 1960.
E-mail address: k-okmt@nih.go.jp (K. Okamoto).

0166-0934/$ – see front matter © 2010 Elsevier B.V. All rights reserved.
doi:10.1016/j.jviromet.2010.05.016

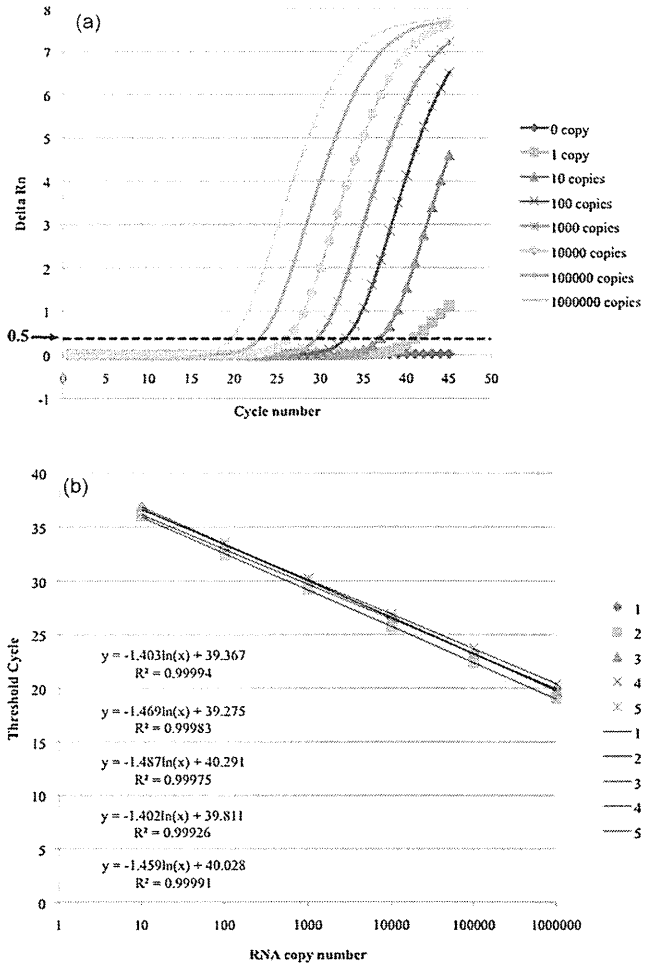

Fig. 1. Determination of the cut-off values (a) and standard curves (b). Ten-fold dilutions of standard RNA were used with the TaqMan assay. (a) Each sample was amplified in triplicate. The broken line indicates $\Delta R_n = 0.5$. (b) Five independent experiments were performed in triplicate. Each numerical expression represents a regression line, and R^2 indicates the coefficient of determination.

ing TaqMan primers and probes using Primer Express Software Ver. 3 (Applied Biosystems, Foster City, CA). The sequence of the probe was 5′-CCGTCGGCAGTTGG-3′ (encoding nt 93–106), that of the forward primer was 5′-CCTAHYCCCATGGAGAAACTCCT-3′ (nt 32–54), and that of the reverse primer was 5′-AACATCGCGCACTTCCCA-3′ (nt 143–160). The reporter probe was conjugated with 6-carboxyfluorescein and minor groove binder at the 5′ and 3′ termini, respectively.

To determine the cut-off values for the TaqMan assay, synthesized RNA in vitro (consisting of 1–782 nt of TO336 wt-type) was quantified by OD_{260}, and a 10-fold dilution series was prepared (from 2.0×10^5 to 2.0×10^{-1} copies/μl) and applied to the TaqMan assay (Fig. 1a). The assay was performed by using a TaqMan RNA-to-C_T 1-Step Kit (Applied Biosystems) in a total volume of 20 μl, which contained a final concentration of 900 nM sense and antisense primers, 250 nM probe, 1× TaqMan RT Enzyme Mix, and 1× TaqMan RT-PCR Mix. The kinetics of cDNA amplification were monitored using an Applied Biosystems 7500 Real-Time PCR System (Applied Biosystems) under the conditions of 48 °C for 15 min, 95 °C for 10 min, and 45 cycles of 95 °C for 15 s and 60 °C for 1 min. This assay was carried out in triplicate for each sample, including a no-template control. Test samples were considered positive if amplification with a threshold cycle (Ct) value <40 and ΔR_n signal >0.5 were seen in all of the triplicate reactions. Five distinct sets of 10-fold-diluted standard RNA samples (1.0×10^6 to 1 copies/reaction) were examined to estimate the dynamic range of this assay. Although above 10 copies/reaction were detected in all samples, 1 copy/reaction was detected in 47% of samples (Table 1). The standard curve from 1 to 1.0×10^6 copies/reaction did not satisfy a linear relationship of $R^2 > 0.99$ (data not shown); therefore, the data of one copy/reaction was omitted from the standard curve. Log-linear regression plots showed a strong linear relationship ($R^2 > 0.99$) between the log of the starting copy number (from 10 to 1.0×10^6 copies) and the Ct values (Fig. 1b). All standard curves showed a similar slope and intercept, and the reproducibility of the standard curve was reliable, at least in the range from 10 to 1.0×10^6 copies/reaction. These results indicate that the dynamic range of this assay was from 10 to at least 1.0×10^6 copies/reaction.

Thirteen RV genotypes have been recognized to date (WHO, 2007b), all belonging to only one serotype. These genotypes are classified into two clades: clade1 and clade 2. Clade 2 has not been reported in Japan, except for Rvi/OSAKA.JPN/11.07 (2B), isolated in 2007. Few studies using real-time PCR for detection of the RV genome have compared the sensitivity and specificity between the viral genotypes or strains using RNA extracted from viral stocks, although several investigators have used real-time PCR for RV diagnosis (Abernathy et al., 2009; Hübschen et al., 2008; Rajasundari et al., 2008; Zhao et al., 2006). To investigate the sensitivity and specificity of the TaqMan assay for various viruses, 10 RV strains consisting of five genotypes (1a, 1B, 2B, 1D and 1j), which included vaccine strains (Shishido and Ohtawara, 1976) that have been isolated, propagated, and titrated in our laboratory, were examined using this assay, and the results were compared with a conventional RT-PCR. The viral RNA was prepared from 140 μl of culture medium of RK-13 cells infected with each RV, using a QIAamp Viral RNA Mini Kit (QIAGEN, Tokyo, Japan) according to the manufacturer's protocol, extracted with 70 μl of elution buffer, and each 5 μl of eluted sample was subjected to the TaqMan assay and the conventional RT-PCR. The conventional RT-PCR conditions are described below.

For amplifying an 851-nt region in the E1 coding region (nt 8702–9553) using a primer set F1 (5′-CGACGCGGCCTGCTGGGGC) and R9 (5′-AGGTCTGCCGGGTCTCCGAC), RT-PCR was performed with One-Step RT-PCR Kit (QIAGEN) according to the manufacturer's protocol, except that the total reaction volume and concentration of the primers were altered to 25 μl and 0.3 μM, respectively. After carrying out the RT reaction for 30 min at 55 °C and denaturation for 15 min at 95 °C, the reaction mix-

Table 1
Detection limit of the TaqMan assay using a series of synthesized standard RNA.

Standard RNA (copies/reaction)	Number of positive samples/number of tested samples					Positive (%)
	1	2	3	4	5	
10^6	3/3	3/3	3/3	3/3	3/3	100%
10^5	3/3	3/3	3/3	3/3	3/3	100%
10^4	3/3	3/3	3/3	3/3	3/3	100%
10^3	3/3	3/3	3/3	3/3	3/3	100%
10^2	3/3	3/3	3/3	3/3	3/3	100%
10	3/3	3/3	3/3	3/3	3/3	100%
1	0/3	2/3	0/3	3/3	2/3	47%

tures were incubated for 35 cycles of 94 °C for 30 s, 62 °C for 30 s, and 72 °C for 1 min, followed by 72 °C for 10 min. The RT-PCR product (0.5 μl) was used as a template for a nested PCR with 2 mM $MgCl_2$, 50 mM KCl, 25 mM TAPS buffer (pH 9.3), 200 μM sense (5′-CAGCACCCTCACAAGACCGTC-3′) and anti-sense (5′-CACAGCAGTGGTGTGTGTGCC-3′) primers, and 0.025 U Ex Taq polymerase (TaKaRa Bio, Shiga, Japan). The cycling conditions were as follows: 98 °C for 30 s, and 30 cycles of 98 °C for 10 s and 68 °C for 1 min. The PCR products were resolved on a 1% agarose gel and visualized by ethidium bromide staining. As a result, at least 1 pfu of RV could be detected in Rvi/OSAKA.JPN/11.07 (2B), SRL6.97 (1D), and Osaka' 94 (1D) strains by the TaqMan assay (Table 2), although a greater viral load was required in the other viral strains (from 10 to 100 pfu). On the other hand, at least 10 pfu of the virus was required for detection by the conventional RT-PCR, and for the Kagoshima' 04 strain (1j), as much as 1000 pfu of the virus was required. Thus, the novel real-time PCR had about 10-fold greater sensitivity compared with the conventional RT-PCR. Although the conventional RT-PCR amplified a relatively long region (851 bp), the sensitivity of this method was almost identical to that of another RT-PCR amplifying 481 bp (data not shown). Conventional RT-PCR amplifying the 851-nt sequencing region in the E1 coding region could be used for direct genotyping. Thus, the conventional RT-PCR is also thought to be useful for rapid genotyping. The sequences of the target region for the TaqMan assay were identical among genotype 1a strains (data not shown). The reason for the low sensitivity of the TaqMan assay for the TO336 wild-type and the Matsuura vaccine strains is unknown.

It is necessary for monitoring to confirm the morbidity of rubella precisely, and it is especially important to distinguish rubella from other infectious diseases. Clinical diagnosis of rubella is sometimes confused with measles, HHV-6, and parvovirus B19, because they have similar major symptoms to rubella (WHO, 2007a). Therefore, to exclude the possibility of false-positive results for other viruses, measles viral RNA (strains SA203, Yamagata, IC-B, YS-4, Edmonston, and Toyoshima, kindly provided by Dr. Seki, Department of Virology III, National Institute of Infectious Diseases), HHV-6 type A DNA (kindly provided by Dr. Inoue, Department of Virology I, National Institute of Infectious Diseases), and parvovirus B19 DNA (kindly provided by Dr. Okada, Department of Blood, National Institute of Infectious Diseases) were examined (Table 3). Measles virus strains used in this study included wild-type isolates with various genotypes that are found frequently in Japan or Asia (D5, D9, and H1) (CDC, 2005), a vaccine strain (A), and a laboratory strain (D3). Although the amount of template in the measles virus and parvovirus B19 was not known precisely, the samples were confirmed as positive by conventional RT-PCR or PCR-specific for each virus (data not shown). These viral RNAs or DNAs were not detected by the probe or primers used in this study.

It is difficult to obtain an adequate number of clinical samples from patients suspected of rubella infection in Japan, because the morbidity rate decreased significantly in recent years. Therefore, to mimic the detection of viral RNA extracted from clinical specimens, a spike test was performed as an alternative resource. Throat swabs from healthy donors collected in a Universal Viral Transport (UVT) medium (BD, Franklin Lakes, NJ) were added to 1, 10, 10^2, and 10^3 pfu of three viral strains, TO336 vaccine (1a), Osaka' 94 (1D), and Kagoshima' 04 (1j), and subjected to the TaqMan assay and the conventional RT-PCR. Ten pfu of all viruses could be detected by the TaqMan assay (Table 4). However, even 10^3 pfu of each virus could not be detected by the conventional RT-PCR. The TaqMan assay detected viral RNA from the spiked test samples to almost the same degree as with a viral culture medium. This showed that neither the RNA extraction step nor the TaqMan assay was affected by the presence of contaminants included in clinical specimens (i.e., throat swabs).

Table 2
Sensitivity of the TaqMan and conventional RT-PCR assay.

Strain	Genotype	Viral dose (pfu)											
		10^4		10^3		10^2		10^1		10^0		10^{-1}		10^{-2}	
		TaqMan	RT-PCR	TaqMan	RT-PCR	TaqMan	RT-PCR	TaqMan	RT-PCR	TaqMan	RT-PCR	TaqMan	RT-PCR	TaqMan	RT-PCR
TO336 wild	1a	27.5 ± 0.25	N/A	31.3 ± 0.30	+	35.4 ± 0.25	+	40.0<	−	40.0<	−	40.0<	N/A	40.0<	N/A
TO336 vaccine	1a	24.2 ± 0.26	N/A	28.2 ± 0.17	+	31.8 ± 0.26	+	35.4 ± 0.15	−	40.0<	−	40.0<	N/A	40.0<	N/A
Matsuura wild	1a	26.6 ± 0.34	N/A	30.3 ± 0.52	+	34.1 ± 0.51	+	37.5 ± 0.50	+	40.0<	−	40.0<	N/A	40.0<	N/A
Matsuura vaccine	1a	28.1 ± 0.48	N/A	31.6 ± 0.39	+	35.5 ± 0.53	+	40.0<	−	40.0<	−	40.0<	N/A	40.0<	N/A
SRL 8.79	1B	25.0 ± 0.94	N/A	28.6 ± 0.86	+	32.4 ± 0.79	+	36.0 ± 1.00	+	40.0<	−	40.0<	N/A	40.0<	N/A
Rvi/OSAKA.JPN/11.07	2B	22.1 ± 0.42	N/A	25.2 ± 0.29	+	28.9 ± 0.21	+	32.7 ± 0.39	+	36.2 ± 0.15	−	40.0<	N/A	40.0<	N/A
SRL 6.97	1D	24.4 ± 0.34	N/A	27.5 ± 0.24	+	31.0 ± 0.19	+	35.0 ± 0.08	−	38.8 ± 0.15	−	40.0<	N/A	40.0<	N/A
Osaka' 94	1D	23.7 ± 0.31	N/A	27.3 ± 0.22	+	31.0 ± 0.21	+	34.6 ± 0.35	+	38.5 ± 1.11	−	40.0<	N/A	40.0<	N/A
Miyazaki' 01	1j	25.3 ± 0.16	N/A	29.0 ± 0.19	+	32.9 ± 0.21	+	36.5 ± 0.22	+	40.0<	−	40.0<	N/A	40.0<	N/A
Kagoshima' 04	1j	26.3 ± 0.18	N/A	29.8 ± 0.19	+	33.5 ± 0.10	−	37.3 ± 0.41	−	40.0<	−	40.0<	N/A	40.0<	N/A

Table 3
Specificity of the TaqMan assay.

Virus			Amount of template	Ct	Result
RV					
	TO336 wild	1a	100 pfu	35.4 ± 0.25	Pos.
	TO336 vaccine	1a	100 pfu	31.8 ± 0.26	Pos.
	Matsuura wild	1a	100 pfu	34.1 ± 0.51	Pos.
	Matsuura vaccine	1a	100 pfu	35.5 ± 0.53	Pos.
	SRL 8.79	1B	100 pfu	32.4 ± 0.79	Pos.
	Rvi/OSAKA.JPN/11.07	2B	100 pfu	28.9 ± 0.21	Pos.
	SRL 6.97	1D	100 pfu	31.0 ± 0.19	Pos.
	Osaka' 94	1D	100 pfu	31.0 ± 0.21	Pos.
	Miyazaki' 01	1j	100 pfu	32.9 ± 0.21	Pos.
	Kagoshima' 04	1j	100 pfu	33.5 ± 0.10	Pos.
MV					
	SA203	D5	N/A	40.0<	Neg.
	Yamagata	D9	N/A	40.0<	Neg.
	IC-B	D3	N/A	40.0<	Neg.
	YS-4	H1	N/A	40.0<	Neg.
	Ed	A	N/A	40.0<	Neg.
	Toyoshima	A	N/A	40.0<	Neg.
Others					
	HHV-6 U1102	A	0.5 μg of DNA	40.0<	Neg.
	HHV-6 Z29	B	0.5 μg of DNA	40.0<	Neg.
	Parvovirus B19		N/A	40.0<	Neg.

Table 4
Spike test for detection of RV in throat swabs.

Strain	Genotype	Viral dose (pfu)			
		10^3		10^2	
		TaqMan	RT-PCR	TaqMan	RT-PCR
TO336 vaccine	1a	29.4 ± 0.13	–	33.1 ± 0.11	–
Osaka' 94	1D	27.8 ± 1.12	–	32.1 ± 1.33	–
Kagoshima' 04	1j	28.5 ± 1.12	–	32.7 ± 1.45	–

Table 5
Detection of RV in clinical specimens by TaqMan assay.

Individuals	Specimens	TaqMan #1	Ct	TaqMan #2	Ct	RT-PCR	Virus isolation
1	Oral fluid	Pos.	34.9	Pos.	35.7	Pos.	Pos.
2	Oral fluid	Pos.	39.4	Pos.	39.3	Neg.	Pos.
3	Oral fluid	Pos.	38.4	Pos.	37.9	Neg.	Pos.
4	Oral fluid	Pos.	36.1	Pos.	36.7	Pos.	Pos.
5	Oral fluid	Pos.	38.5	Pos.	39.1	Neg.	Pos.
6	Oral fluid	Pos.	31.6	Pos.	33.7	Neg.	Pos.

To compare the sensitivity of the novel TaqMan assay in clinical specimens with the conventional RT-PCR, six oral fluids collected from an outbreak of rubella in 2004 in Japan were tested using the TaqMan assay (TaqMan #1) and conventional RT-PCR. All samples were confirmed as positive by the conventional RT-PCR after passages in culture. As a result, all specimens (6/6) were positive using the TaqMan assay, although two of the six samples were positive using the conventional RT-PCR (Table 5). The same samples were also subjected to another TaqMan assay (TaqMan #2), which has been reported previously (Zhu et al., 2007; Abernathy et al., 2009). However, no amplification was detected both in the negative control and in the positive control using the TaqMan #2 method (data not shown). When the primers and probe were used with the same reagent in this study (TaqMan RNA-to-C_T 1-Step Kit), amplification signals were obtained. Under these conditions, all specimens (6/6) were also found to be positive, with similar Ct values to the TaqMan #1 method (Table 5). Although it was unclear why the primers and probe of TaqMan #2 method did not function under the assay conditions described previously, the primers and probe could function equally well as those of the novel TaqMan method (TaqMan #1) under the assay condition used in TaqMan #1 method. The TaqMan assay used in this study was more reliable, because it was confirmed that this assay could detect various viral strains sensitively and did not cross-react with other viral RNAs causing similar symptoms as rubella.

Detection of viral RNA in oral fluid seems to be more suitable for rapid diagnosis of rubella. WHO does not recommend viral genome detections for laboratory confirmation, probably due to the possibility of laboratory contamination and cross-contamination when performing RT-PCR followed by nested PCR. However, given the lower risk of contamination using real-time PCR and its higher sensitivity compared with conventional RT-PCR, the former technique is concluded to be more suitable for rapid diagnosis. The new real-time PCR assay described above was able to detect at least 10 copies of RV RNA and 1 pfu of virus. This TaqMan PCR assay is considered to be useful for rapid diagnosis and screening of rubella when used in conjunction with conventional RT-PCR.

Acknowledgments

This work was supported by Research Programs for Regulatory Science from the Ministry of Health, Labour and Welfare, Japan.

We thank Dr. F. Kobune and Dr Y. Umino for providing viruses, and Tochigi Prefectural Institute of Public Health and Environmental Science and Miyazaki Prefectural Institute of public Health and Environment for collecting specimens. We thank Dr. Morikawa, Department of Virology I, Laboratory of Special Pathogens, and Dr. Shirato, Department of Virology III, Laboratory of Acute Viral Respiratory Infections and Cytokines for their helpful discussions.

Ethics Committee approval for the collection of throat swabs from the authors for the use as controls was not required by the National Institute of Infectious Diseases.

References

Abernathy, E., Cabezas, C., Sun, H., Zheng, Q., Chen, M.H., Castillo-Solorzano, C., Ortiz, A.C., Osores, F., Oliveira, L., Whittembury, A., Andrus, J.K., Helfand, R.F., Icenogle, J., 2009. Confirmation of rubella within 4 days of rash onset: comparison of rubella virus RNA detection in oral fluid with immunoglobulin M detection in serum or oral fluid. J. Clin. Microbiol. 48, 182–188.

CDC, 2005. Global Measles and Rubella Laboratory Network, January 2004–June 2005. Morb. Mortal. Wkly. Rep. 54, 1100–1104.

CDC, 2008. Recommendations from an ad hoc Meeting of the WHO Measles and Rubella Laboratory Network (LabNet) on use of alternative diagnostic samples for measles and rubella surveillance. Morb. Mortal. Wkly. Rep. 57, 657–660.

Cooray, S., Warrener, L., Jin, L., 2006. Improved RT-PCR for diagnosis and epidemiological surveillance of rubella. J. Clin. Virol. 35, 73–80.

Frey, T.K., 1994. Molecular biology of rubella virus. Adv. Virus Res. 44, 69–160.

Hübschen, J.M., Kremer, J.R., De Landtsheer, S., Muller, C.P., 2008. A multiplex TaqMan PCR assay for the detection of measles and rubella virus. J. Virol. Methods 149, 246–250.

Jin, L., Thomas, B., 2007. Application of molecular and serological assays to case based investigations of rubella and congenital rubella syndrome. J. Med. Virol. 79, 1017–1024.

Liang, Y., Gillam, S., 2000. Mutational analysis of the rubella virus nonstructural polyprotein and its cleavage products in virus replication and RNA synthesis. J. Virol. 74, 5133–5141.

Oker-Blom, C., Ulmanen, I., Kääriäinen, L., Pettersson, R.F., 1984. Rubella virus 40S genome RNA specifies a 24S subgenomic mRNA that codes for a precursor to structural proteins. J. Virol. 49, 403–408.

Pugachev, K., Abernathy, E., Frey, T., 1997. Improvement of the specific infectivity of the rubella virus (RUB) infectious clone: determinants of cytopathogenicity induced by RUB map to the nonstructural proteins. J. Virol. 71, 562–568.

Rajasundari, T.A., Sundaresan, P., Vijayalakshmi, P., Brown, D.W., Jin, L., 2008. Laboratory confirmation of congenital rubella syndrome in infants: an eye hospital based investigation. J. Med. Virol. 80, 536–546.

Shishido, A., Ohtawara, M., 1976. Development of attenuated rubella virus vaccines in Japan. Jpn. J. Med. Sci. Biol. 29, 227–253.

Tipples, G., Hamkar, R., Mohktari-Azad, T., Gray, M., Ball, J., Head, C., Ratnam, S., 2004. Evaluation of rubella IgM enzyme immunoassays. J. Clin. Virol. 30, 233–238.

Vyse, A., Jin, L., 2002. An RT-PCR assay using oral fluid samples to detect rubella virus genome for epidemiological surveillance. Mol. Cell. Probes 16, 93–97.

WHO, 2007a. Manual for the Laboratory Diagnosis of Measles Virus Infection, Second edition. World Health Organization, Department of Immunization, Vaccines and Biologicals, Geneva.

WHO, 2007b. Update of standard nomenclature for wild-type rubella viruses, 2007. Wkly. Epidemiol. Rec. 82, 216–222.

Yao, J., Yang, D., Chong, P., Hwang, D., Liang, Y., Gillam, S., 1998. Proteolytic processing of rubella virus nonstructural proteins. Virology 246, 74–82.

Zhao, L.H., Ma, Y.Y., Wang, H., Zhao, S.P., Zhao, W.M., Li, H., Wang, L.Y., 2006. Establishment and application of a TaqMan real-time quantitative reverse transcription-polymerase chain reaction assay for rubella virus RNA. Acta Biochim. Biophys. Sin. (Shanghai) 38, 731–736.

Zhu, Z., Xu, W., Abernathy, E., Chen, M., Zheng, Q., Wang, T., Zhang, Z., Li, C., Wang, C., He, W., Zhou, S., Icenogle, J., 2007. Comparison of four methods using throat swabs to confirm rubella virus infection. J. Clin. Microbiol. 45, 2847–2852.

Vaccine 29 (2011) 1863–1873

Contents lists available at ScienceDirect

Vaccine

journal homepage: www.elsevier.com/locate/vaccine

Elucidation of the full genetic information of Japanese rubella vaccines and the genetic changes associated with *in vitro* and *in vivo* vaccine virus phenotypes

Noriyuki Otsuki*, Hitoshi Abo, Toru Kubota, Yoshio Mori, Yukiko Umino, Kiyoko Okamoto, Makoto Takeda, Katsuhiro Komase

Department of Virology 3, National Institute of Infectious Diseases, Gakuen 4-7-1, Musashimurayama, Tokyo 208-0011, Japan

ARTICLE INFO

Article history:
Received 11 November 2010
Received in revised form 5 January 2011
Accepted 8 January 2011
Available online 18 January 2011

Keywords:
Rubella
Temperature-sensitive
Genome
Marker test
Attenuation

ABSTRACT

Rubella is a mild disease characterized by low-grade fever, and a morbilliform rash, but causes congenital defects in neonates born from mothers who suffered from rubella during the pregnancy. After many passages of wild-type rubella virus strains in various types of cultured cells, five live attenuated rubella vaccines were developed in Japan. An inability to elicit anti-rubella virus antibodies in experimentally infected animals was used as an *in vivo* marker phenotype of Japanese rubella vaccines. All Japanese rubella vaccine viruses exhibit a temperature-sensitive (ts) phenotype, and replicate very poorly at a high temperature. We determined the entire genome sequences of three Japanese rubella vaccines (Matsuba, TCRB19, and Matsuura), thereby completing the sequencing of all five Japanese rubella vaccines. In addition, the entire genome sequences of three vaccine progenitors were determined. Comparative nucleotide sequence analyses revealed mutations that were introduced into the genomes of the TO-336 and Matsuura vaccines during their production by laboratory passaging. Analyses involving cellular expression of viral P150 nonstructural protein-derived peptides revealed that the N1159S mutation conferred the ts phenotype on the TO-336 vaccine, and that reduced thermal stability of the P150 protease domain was a cause of the ts phenotype of some rubella vaccine viruses. The ts phenotype of vaccine viruses was not necessarily correlated with their inability to elicit humoral immune responses in animals. Therefore, the molecular mechanisms underlying the inability of these vaccines to elicit humoral responses in animals are more complicated than the previously considered mechanism involving the ts phenotype as the major cause.

1. Introduction

Rubella is a communicable and ordinarily mild disease that is characterized by low-grade fever, a short-lived morbilliform rash, and lymphadenopathy [1]. A German physician originally designated this disease 'German measles', since it resembles measles but is much less severe [1]. Arthralgia and arthritis are common complications of rubella, particularly in adolescent and adult females. Rubella has received much attention following a report that congenital cataracts were associated with rubella infection of mothers during pregnancy [2]. Subsequent studies indicated that sensorineural hearing loss and cardiovascular defects are also common in neonates born from mothers who suffered from rubella, especially during the early phase of pregnancy [1].

Rubella virus (RuV) was first isolated in 1962 [3,4], and belongs to the genus *Rubivirus* in the family *Togaviridae*. After many passages of wild-type (wt) RuV strains in various types of cultured cells, live attenuated rubella vaccines were developed [1,5,6]. The first rubella vaccine was licensed in the United States in 1969 [7]. A total of nine vaccines (HPV-77, RA27/3, Cendehill, BRD-2, Matsuba, TCRB19, KRT, Matsuura, and TO-336) have been developed to date [1,7]. Among these, five vaccines were developed in Japan [6].

An increased growth rate in certain cultured cells has been used as an *in vitro* marker phenotype of Japanese rubella vaccines [6]. In addition, an inability to elicit anti-RuV antibodies in experimentally infected guinea pigs and rabbits has been used as an *in vivo* marker phenotype of Japanese rubella vaccines [6]. The Minimum Requirements for Biological Products (MRBP) announced by the Ministry of Health, Labour and Welfare, Japan, defines the *in vivo* phenotype as a marker phenotype of rubella vaccines [8,9]. All lots of commercially used Japanese rubella vaccines must receive a national test by the National Institute of Infectious Diseases, Japan, to verify this phenotype as a marker test [8,9]. Later, it was recognized that all Japanese rubella vaccines exhibit a temperature-sensitive (ts) phenotype, meaning that they replicate very poorly at a high temperature (39 °C), whereas wt strains can replicate well at that temperature [5]. Although understanding of the molecular bases for acquisition of these *in vitro* and *in vivo* vaccine virus pheno-

* Corresponding author. Tel.: +81 42 561 0771; fax: +81 42 562 8941.
E-mail address: otsuki@nih.go.jp (N. Otsuki).

0264-410X/$ – see front matter © 2011 Elsevier Ltd. All rights reserved.
doi:10.1016/j.vaccine.2011.01.016

types is crucial for quality control of vaccines, they have been poorly elucidated. In the present study, we performed various analyses to elucidate the genetic changes introduced into the genomes of rubella vaccines during passages under laboratory conditions and to show importance of these changes in determining the *in vitro* and *in vivo* vaccine virus phenotypes. Our data in the present study provide basic and solid information for the genetic changes of rubella vaccines as well as a novel insight into the understanding of molecular bases for the vaccine phenotypes.

2. Materials and methods

2.1. Cells and viruses

RK13 cells were cultured in Eagle's minimal essential medium (MEM) supplemented with 8% bovine serum. After infection with RuV, the cells were cultured in MEM containing 2% bovine serum. When transfected with plasmids, the cells were cultured in Dulbecco's modified Eagle's medium (DMEM) supplemented with 10% fetal bovine serum (FBS) and 0.1 mM non-essential amino acids.

Five licensed vaccines (KRT, Matsuba, TCRB19, TO-336, and Matsuura) were passaged once or twice in RK13 cells to obtain sufficient amounts of stocks. These vaccines were termed as KRT, Matsuba.vac, TCRB19, TO-336.vac, and Matsuura.vac, respectively, in the present study. Three wt strains, TO-336.GMK5, Matsuba.GMK3, and Matsuura.B3, isolated in Japan in the late 1960s were also passaged in RK13 cells once or twice to obtain sufficient amounts of virus stocks. The wt RVi/Hiroshima.JPN/01.03 strain isolated in Japan in 2003 was passaged four times in RK13 cells. A TO-336.vac-derived mutant clone that replicated well at a high temperature was generated as follows. RK13 cells were infected with TO-336.vac and incubated at 39 °C. A clone that replicated well at this temperature was plaque-purified and propagated in RK13 cells at 39 °C. The obtained clone was designated TO-336.rev.

2.2. Sequencing

Viral RNAs were extracted from each virus stock using a High Pure Viral RNA Kit (Roche Diagnostics GmbH, Mannheim, Germany) according to the manufacturer's instructions. Several cDNA fragments covering the entire virus genome were amplified using a One-step RT-PCR Kit (Qiagen KK, Tokyo, Japan). The primers used for amplification will be provided upon request. To determine the 5′ terminus of each viral genome, a 5′ RACE system (Invitrogen, Carlsbad, CA) was used. To amplify the 3′ terminus of the viral genome, an RNA PCR Kit (AMV) ver. 3.0 (Takara Bio, Shiga, Japan) was used with an oligo (dT) adaptor primer. The PCR products were purified using a QIAquick Gel Extraction Kit (Qiagen KK) and a QIAquick PCR Purification Kit (Qiagen KK). The nucleotide sequences of the purified PCR products were determined using a Big Dye Terminator v3.1 Cycle Sequencing Kit (Applied Biosystems, Foster City, CA) and a capillary sequencer. Some PCR products were cloned into the pCR2.1 vector (Invitrogen), and the nucleotide sequences of more than three clones were analyzed to determine a consensus sequence.

2.3. Sequence data analysis

The entire genome sequences of 13 RuV strains were used for comparisons. Data for seven RuV strains, Therien [10] (GenBank M15240), RA27/3 [11] (GenBank L78917), RVi/Matsue.JPN/68 [12] (GenBank AB222609), TO-336wt [13] (GenBank AB047330), TO-336.vac [13] (GenBank AB047329), M33 [11,14] (GenBank X72393 and X05259), and KRT [12] (GenBank AB222608) were reported previously. Corrected nucleotide sequence data were used for the Therien and M33 strains [11], rather than the original data (GenBank M15240, X72393, and X05259). The entire genome nucleotide sequences of six RuV strains, TCRB19, Matsuba.GMK3, Matsuura.B3, Matsuura.vac, TO-336.GMK5, and Matsuba.vac, were determined in the present study, and registered in GenBank under accession numbers AB588188, AB588189, AB588190, AB588191, AB588192, and AB588193, respectively. Analyses were performed using the GENETYX-MAC ver. 13.0.14 software (Genetyx, Tokyo, Japan).

2.4. Phylogenic analysis

The phylogenic relationships of the RuV strains were analyzed by drawing a neighbor-joining tree with a kimura-2-parameter model with 739 nucleotides (nt) of the E1 regions of 44 RuV strains using a CLUSTALW ver. 1.83 application (http://www.ddbj.nig.ac.jp/Welcome-j.html). These 739 nt correspond to the minimum acceptable window defined by the World Health Organization [15]. The reliability of the tree was estimated with 1000 iterations of bootstrapping. Another phylogenic tree was similarly constructed using the entire genome sequences of six RuV strains and the neighbor-joining method with a kimura-2-parameter model.

2.5. Growth kinetics analysis

Monolayers of RK-13 cells in 12-well plates were incubated with RuV strains at a MOI of 0.01 for 1 h. After the incubation, the cells were washed three times with phosphate-buffered saline and cultured in 1 ml of MEM containing 2% bovine serum at 35 °C or 39 °C. The culture medium was collected at 0, 1, 2, 3, and 5 days post-infection (p.i.). The virus titers were determined by plaque assays.

2.6. Plaque assay

Monolayers of RK13 cells in 6-well plates were incubated with 0.1 ml of samples that had been serially diluted by 10-fold for 1 h at room temperature. After the incubation, the cells were cultured in 3 ml of MEM containing 2% bovine serum, 0.5% agarose, and 40 μg/ml DEAE-dextran (0.5% agarose-MEM) at 35 °C for 7 days. After this culture period, 2 ml of 0.5% agarose-MEM containing 0.01% neutral red was overlaid on each well. The number of plaques were counted at 2 or 3 days after this procedure.

2.7. Plasmid construction

Plasmids encoding nonstructural protein (NSP)-derived peptides corresponding to amino acid positions 994–1548 ($NSP_{994-1548}$) [16] were constructed as follows. First-strand cDNAs were synthesized from purified viral RNA extracts from the TO-336.vac and KRT strains using SuperScript III reverse transcriptase (Invitrogen) and the 1548 reverse primer (5′-TATGAATTCGCCTACATGGATGCAGGC-3′) [16]. DNA fragments spanning nucleotide positions 994–1548 of the RuV genome were amplified by PCR using the 1548 reverse primer and the 994 forward primer (5′-AATGGATCCATGGACCACCGCCCGGCTGC-3′) [16]. The amplified DNA fragments were inserted into the mammalian cell expression plasmid pCMV-3tag-1a (Stratagene, Carlsbad, CA), in the downstream of a CMV promoter, using restriction enzyme recognition sites for *BamH*I and *EcoR*I, such that $NSP_{994-1548}$ was expressed as a peptide fused with three FLAG tags. Single point mutations were introduced into pCMV-3tag-1a encoding $NSP_{994-1548}$ using a KOD-plus- Mutagenesis Kit (Toyobo, Osaka, Japan).

2.8. Protein expression using plasmids and detection by immunoblotting

RK13 cells were transfected with pCMV-3tag-1a encoding $NSP_{994-1548}$ using the Lipofectamine LTX Plus reagent (Invitrogen) and cultured at 35 °C or 39 °C for 1 day or 3 days. In another experiment, transfected cells were cultured at 35 °C for 1 day, and subsequently, *de novo* protein synthesis was blocked by culturing the cells in medium containing 0.1 mg/ml cycloheximide at 35 °C or 39 °C for 2 days. After cell lysis, polypeptides were separated by electrophoresis in a polyacrylamide gel (10–20% gradient) in the presence of 0.1% sodium dodecyl sulfate and transferred onto nitrocellulose membranes. The membranes were incubated with anti-FLAG or anti-tubulin (clone B-5-1-2) antibodies (Sigma) followed by incubation with a peroxidase-conjugated secondary antibody. Peptides were then detected using an ECL Advance Western Blotting Detection Kit (GE Healthcare, Buckinghamshire, UK). The signal intensities were quantified using an LAS 1000plus Image Analyzer and the Image Gauge software (Fuji Film, Tokyo, Japan).

2.9. Detection of antibody titers in animals infected with RuV as a marker test

Specific pathogen-free female Hartley guinea pigs (weighing 300–400 g; 4, 8, or 12 animals per group) were infected subcutaneously with 5000 PFU of RuV. At 5 weeks p.i., the animals were euthanized and blood samples were obtained. The serum hemagglutination inhibition (HI) antibody titers were determined using goose erythrocytes and the hemagglutination antigen of RuV (Denka Seiken, Tokyo, Japan). Prior to the analyses, the serum specimens were treated with kaolin to remove nonspecific inhibitors and absorbed with goose erythrocytes to remove nonspecific hemagglutinins. After these treatments, the initial dilution of the samples was 1:8.

3. Results

3.1. TO-336.GMK5 and Matsuura.B3 strains are progenitors of or closely related to the progenitors of the currently used rubella vaccine strains

The growth kinetics of TO-336.GMK5, Matsuba.GMK3, and Matsuura.B3 were analyzed at 35 °C and 39 °C, and compared with those of the vaccine strains. The RVi/Hiroshima.JPN/01.03 wt strain was also evaluated as a control. After infection at 35 °C, all the tested viruses grew well and reached infectious titers that ranged from 10^4 to 10^6 PFU/ml at 5 days p.i. (Fig. 1A). At 39 °C, TO-336.GMK5 and Matsuura.B3 grew productively and were similar to the RVi/Hiroshima.JPN/01.03 wt strain (Fig. 1B). In contrast, all of the vaccine strains showed abortive infections (Fig. 1B). Although Matsuba.GMK3 was able to replicate at 39 °C, its growth was severely restricted (Fig. 1B). These data show that TO-336.GMK5 and Matsuura.B3 have retained wt phenotypes with the capacity to grow at a high temperature, while Matsuba.GMK3 has a ts phenotype, although it is less severe than those of the vaccine strains.

Phylogenic analyses using 739 nt of the E1 regions (nucleotide positions 8731–9469) of 44 RuV strains revealed the relationships of the Matsuba.GMK3, TO-336.GMK5, and Matsuura.B3 strains with other RuV wt and vaccine strains (Fig. 2). The data suggested that TO-336.GMK5 was a direct progenitor strain of the currently used TO-336.vac strain. Similarly, the data indicated that Matsuura.B3 was closely related to a progenitor of the currently used Matsuura.vac strain (Fig. 2). On the other hand, Matsuba.GMK3 was apparently unrelated to the Matsuba.vac strain (Fig. 2).

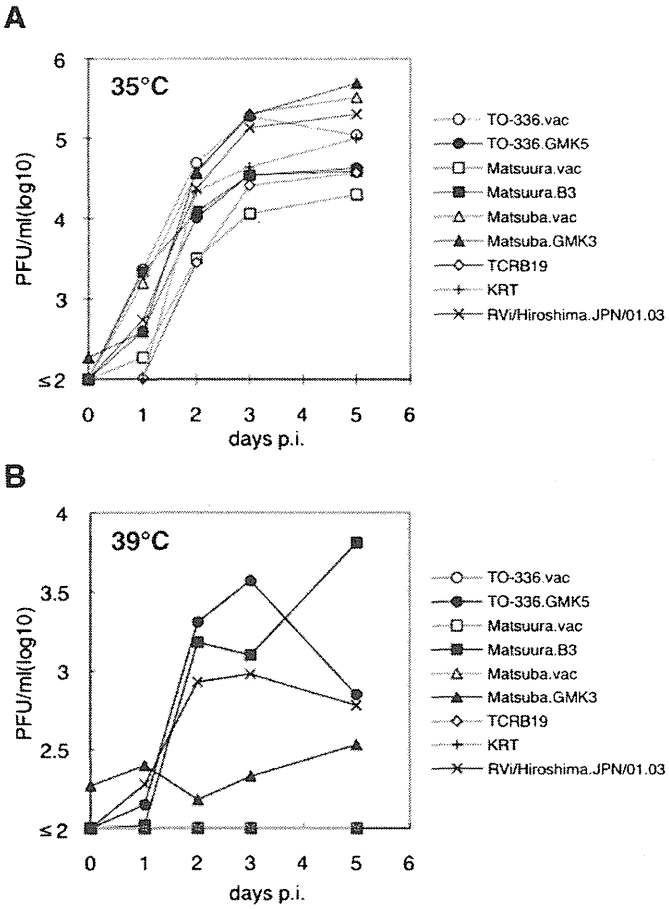

Fig. 1. Growth kinetics of RuV wt strains and vaccines at 35 °C and 39 °C. RK-13 cells were infected with RuV strains at a MOI of 0.01 and incubated at 35 °C (A) or 39 °C (B). The infectious titers of the culture supernatants were determined by plaque assays. Open circles, open squares, open triangles, open diamonds, and crosses indicate TO-336.vac, Matsuura.vac, Matsuba.vac, TCRB19, and KRT, respectively. Filled circles, filled squares, filled triangles, and saltires indicate TO-336.GMK5, Matsuura.B3, Matsuba.GMK3, and RVi/Hiroshima.JPN/01.03, respectively.

3.2. Japanese rubella vaccine strains have deletions in untranslated regions

The entire genome sequences of the TO-336.GMK5, Matsuba.GMK3, and Matsuura.B3 strains and three vaccine strains (Matsuba.vac, TCRB19, and Matsuura.vac) were determined. With the clarification of these sequences, the entire genome sequences became available for 13 RuV strains. These sequences included all five Japanese rubella vaccine (KRT [12], TO-336.vac [13], Matsuura.vac, TCRB19, Matsuba.vac), a US vaccine (RA27/3 [11]), and seven wt strains (Therien [10], M33 [11,14] (Gilliam S., GenBank X72393), TO-336wt [13], RVi/Matsue.JPN/68 [12], TO-336.GMK5, Matsuba.GMK3, and Matsuura.B3). Previous studies have indicated that the genome length of RuV is 9762 nt excluding the 5′ cap and 3′ poly(A) tract, and that the genome consists of a 40-nt 5′ untranslated region (UTR), a 6348-nt open reading frame (ORF) encoding two NSPs (P150 and P90), a 123-nt UTR, a 3189-nt ORF encoding three structural proteins (SPs) (C, E2, and E1), and a 62-nt 3′ UTR [11–13]. The genomes of Matsuba.GMK3, Matsuura.B3, and Matsuura.vac were also 9762 nt in length, and showed the same organization as the previously reported RuV strains [11–13]. On the other hand, the genome lengths of two Japanese vaccine

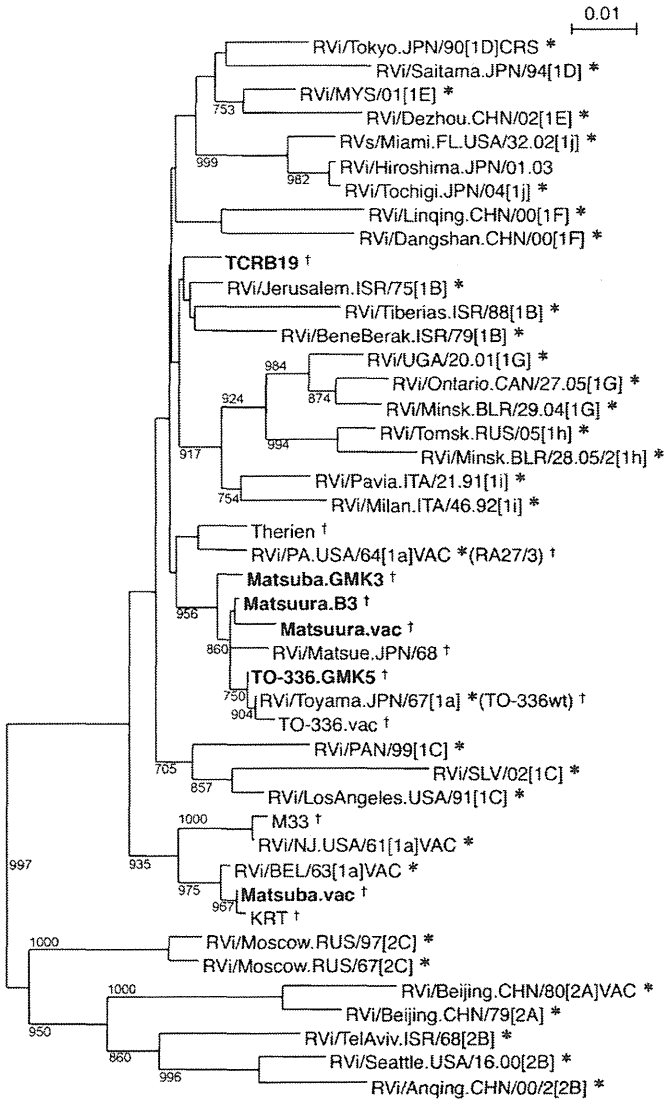

Fig. 2. Phylogenic tree of the 44 RuV strains. A phylogenic tree was drawn on the basis of 739 nt (positions 8731–9469) in the E1 regions of 44 RuV strains using a neighbor-joining method with a kimura-2-parameter model. Boldface characters indicate the strains whose entire genome sequences were determined in the present study. Asterisks indicate World Health Organization reference strains. Daggers indicate strains whose entire genome sequences are currently available. The genotypes based on the World Health Organization nomenclature are shown in square brackets. Bootstrap values above 700 (1000 replications) are shown on the phylogenic tree.

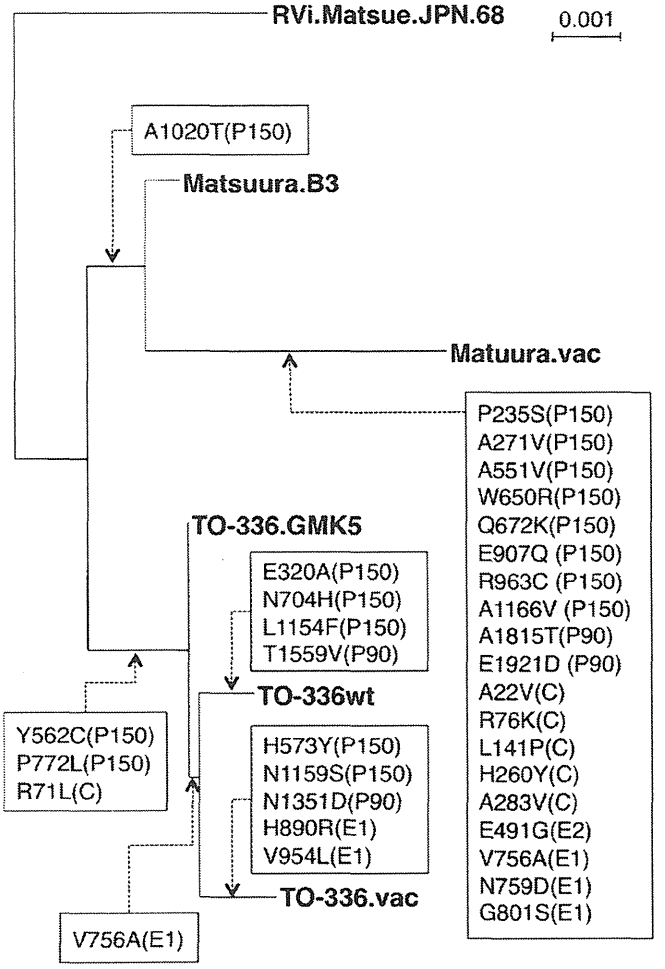

Fig. 3. Phylogenic relationships and amino acid substitutions in the Matsuura and TO-336 RuV strains. A phylogenic tree was drawn on the basis of the entire genome sequences of the Matsuura.B3, Matsuura.vac, TO-336.GMK3, TO-336 wt, TO-336.vac, and RVi/Matsue.JPN68 strains using a neighbor-joining method with a kimura-2-parameter model. The tree was rooted by the RVi/Matsue.JPN68 strain. Amino acid substitutions are indicated in boxes at the predicted points where they were introduced into the Matsuura and TO-336 strains.

strains, Matsuba.vac and TCRB19, were shorter by one nucleotide because of a single deletion in the UTR between the ORFs for the NSPs and SPs (junction UTR). The junction UTR is predicted to form secondary structures with a series of stem-loops [17] and to regulate subgenomic RNA synthesis [18]. Matsuba.vac and TCRB19 had a deletion (Δ) at nucleotide positions 6415 and 6479, respectively. Although neither position appeared to be directly involved in the stem-loop formation, this does not rule out the possibility that these deletions affect the functions of the junction UTR.

3.3. TO-336.vac has acquired six amino acid substitutions under the attenuation process

Kakizawa et al. [13] performed a sequence comparison analysis between TO-336.vac and a TO-336 wt strain (referred to as TO-336wt). They identified 10 amino acid differences between TO-336wt and TO-336.vac [13], while only six amino acid changes were found between TO-336.vac and TO-336.GMK5 (Figs. 3 and 4). A phylogenic tree drawn on the basis of the entire genome sequences revealed that TO-336.GMK5 was a progenitor of both TO-336.vac and TO-336wt (Fig. 4). The data suggested that TO-336wt was a descendant of TO-336.GMK5 with a different passage history from TO-336.vac (Fig. 3). These data are consistent with a previous report regarding the passage history of TO-336wt [19]. A comparison of the amino acid sequences and the phylogenic tree data suggested that TO-336.vac had acquired six substitutions, H573Y and N1159S in P150, N1351D in P90, and V756A, H890R, and V954L in E1, during the passage history of the virus (Fig. 3). N1159S and N1351D were located in the protease domain of P150 and the helicase domain of P90, respectively [20–23] (Fig. 4). Zhou et al. [24] recently reported that a 32-mer peptide region (amino acid positions 1152–1183) within the protease domain acts as a calmodulin-binding domain (CaMBD) that mainly adopts a helical structure and plays crucial roles in the protease activity and virus infectivity. N1159S was located in this helical structure. The V756A substitution in E1 was also found in TO-336wt (Figs. 3 and 4B), and was therefore not reported by Kakizawa et al. [13]. TO-336wt possessed four additional substitutions (E320A, N704H, and L1154F in P150 and T1559V in P90) (Fig. 3). These mutations were unique to TO-336wt

(Fig. 4). Kakizawa et al. [13] reported that TO-336.vac also possesses a unique residue (arginine) at position 501 of P150. However, this residue was not found in our analyses. The TO-336.vac strain used in the present study possessed the same residue as TO-336.GMK5 and TO-336wt at that position.

3.4. Matsuura.vac has acquired 19 amino acid substitutions under the attenuation process

From the nucleotide sequence data, 19 amino acid differences were predicted between Matsuura.B3 and Matsuura.vac

A

		MT																					
		3	42	235	271	289	295	320	323	362	407	427	433	466	473	483	491	503	514	529	541	551	555	562
Wt	M33	K	T	P	A	V	T	E	W	S	S	D	F	L	K	T	A	V	P	R	A	A	L	Y
	Matsuba.GMK5	K	T	P	A	L	T	E	R	S	S	D	F	L	K	T	A	V	P	R	A	A	L	Y
	Matsue.JPN68	K	T	P	A	V	T	E	R	S	G	D	F	F	K	T	A	A	P	R	A	A	L	Y
	TO-336wt	K	T	P	A	V	T	A	R	S	S	D	F	L	K	T	A	A	P	R	A	A	L	C
	TO-336.GMK5	K	T	P	A	V	T	E	R	S	S	D	F	L	K	T	A	A	P	R	A	A	L	C
	Matsuura.B3	K	T	P	A	V	T	E	R	S	S	D	F	L	K	T	A	A	P	R	A	A	L	Y
	Therien	K	T	P	A	V	T	E	R	C	G	D	L	L	K	T	E	V	Q	R	A	A	P	Y
Vac	Matsuba.vac	K	T	P	A	V	A	E	R	S	S	D	F	L	K	T	A	A	P	R	A	A	L	Y
	KRT	K	T	P	A	V	A	E	R	S	S	D	F	L	K	A	A	A	P	R	A	A	L	Y
	TO-336.vac	K	T	P	A	V	T	E	R	S	S	D	F	L	K	T	A	A	P	R	A	A	L	C
	Matsuura.vac	K	T	S	V	V	T	E	R	S	S	D	F	L	K	T	A	A	P	R	A	V	L	Y
	TCRB19	K	T	P	A	V	T	E	R	S	S	D	F	L	Q	T	A	V	P	R	A	A	L	Y
	RA27/3	R	S	P	A	V	T	E	R	S	S	G	F	L	K	T	A	V	P	H	V	A	L	Y

		573	584	604	606	650	672	674	697	699	702	704	715	717	720	722	732	739	740	751	756	758	767	772
Wt	M33	H	G	R	Y	W	K	I	R	T	E	N	G	L	T	P	R	H	S	V	R	Q	V	P
	Matsuba.GMK5	H	E	R	F	W	Q	I	G	A	D	N	G	S	T	S	R	H	L	A	P	A	A	P
	Matsue.JPN68	H	E	R	F	W	Q	I	G	A	D	N	G	S	T	P	R	H	L	A	P	A	A	P
	TO-336wt	H	E	R	F	W	Q	I	G	A	D	H	G	S	T	P	R	H	L	A	P	A	A	L
	TO-336.GMK5	H	E	R	F	W	Q	I	G	A	D	N	G	S	T	P	R	H	L	A	P	A	A	L
	Matsuura.B3	H	E	R	F	W	Q	I	G	A	D	N	G	S	T	P	R	H	L	A	P	A	A	P
	Therien	H	E	R	F	W	Q	I	G	A	D	N	R	S	A	P	R	H	S	A	P	A	A	P
Vac	Matsuba.vac	H	E	R	F	W	Q	V	G	A	D	N	G	L	T	P	R	P	S	V	P	A	A	P
	KRT	H	E	R	F	W	Q	V	G	A	D	N	G	L	T	P	R	P	S	V	P	A	A	P
	TO-336.vac	Y	E	R	F	W	Q	I	G	A	D	N	G	S	T	P	R	H	L	A	P	A	A	L
	Matsuura.vac	H	E	R	F	R	K	I	G	A	D	N	G	S	T	P	R	H	L	A	P	A	A	P
	TCRB19	H	E	C	F	R	Q	I	G	A	D	N	G	P	T	P	R	H	S	A	P	A	A	P
	RA27/3	H	E	R	F	W	Q	I	G	A	D	N	G	S	T	S	C	H	S	A	P	A	A	P

											X								Pro					
		774	775	777	784	790	791	795	799	801	865	874	900	907	930	958	961	963	1002	1007	1020	1042	1115	1117
Wt	M33	T	T	E	H	V	Y	G	S	K	D	I	R	E	R	A	A	R	S	D	A	Y	Q	M
	Matsuba.GMK5	T	S	G	H	A	Y	D	P	K	D	T	Q	E	C	A	A	R	T	D	A	Y	Q	M
	Matsue.JPN68	T	S	G	H	A	Y	D	S	K	D	T	R	E	C	A	A	R	S	D	A	Y	Q	M
	TO-336wt	T	S	G	H	A	Y	D	P	K	D	T	R	E	C	A	A	R	S	D	A	Y	Q	M
	TO-336.GMK5	T	S	G	H	A	Y	D	P	K	D	T	R	E	C	A	A	R	S	D	A	Y	Q	M
	Matsuura.B3	T	S	G	H	A	Y	D	P	K	D	T	R	E	C	A	A	R	S	D	T	Y	Q	M
	Therien	I	P	G	D	A	C	G	S	R	N	T	R	E	C	T	V	R	S	D	A	Y	H	M
Vac	Matsuba.vac	T	S	E	H	V	Y	G	S	K	D	T	R	E	C	A	V	R	S	G	A	H	Q	M
	KRT	T	S	E	H	V	Y	G	S	K	D	T	R	E	C	A	V	R	S	G	A	H	Q	M
	TO-336.vac	T	S	G	H	A	Y	D	P	K	D	T	R	E	C	A	A	R	S	D	A	Y	Q	M
	Matsuura.vac	T	S	G	H	A	Y	D	P	K	D	T	R	Q	C	A	A	C	S	D	T	Y	Q	M
	TCRB19	T	S	G	D	A	Y	G	S	K	D	T	R	E	C	T	A	R	S	D	A	C	Q	M
	RA27/3	T	S	G	D	A	Y	G	S	K	D	T	R	E	R	T	A	R	S	D	A	Y	Q	V

		Pro									Hel										RdRp		
		1140	1154	1159	1166	1177	1190	1191	1199	1209	1337	1351	1393	1403	1466	1497	1559	1583	1639	1767	1815	1921	1979
Wt	M33	V	L	N	A	K	H	E	W	P	I	N	D	A	G	T	T	L	R	T	A	E	N
	Matsuba.GMK5	V	L	N	A	K	H	E	R	P	V	N	D	A	E	T	T	S	R	A	A	E	S
	Matsue.JPN68	V	L	N	A	K	H	E	R	P	V	N	D	A	E	T	T	S	R	A	A	E	S
	TO-336wt	V	F	N	A	K	H	E	R	P	V	N	D	A	E	T	V	S	R	A	A	E	S
	TO-336.GMK5	V	L	N	A	K	H	E	R	P	V	N	D	A	E	T	T	S	R	A	A	E	S
	Matsuura.B3	V	L	N	A	K	H	E	R	P	V	N	D	A	E	T	T	S	R	A	A	E	S
	Therien	A	L	N	A	K	H	E	R	P	V	N	D	R	E	T	T	S	R	A	A	E	S
Vac	Matsuba.vac	V	L	N	A	K	H	E	R	P	V	N	D	A	E	I	T	S	C	A	A	E	S
	KRT	V	L	N	A	K	H	E	R	P	V	N	D	A	E	I	T	S	R	A	A	E	S
	TO-336.vac	V	L	S	A	K	H	E	R	P	V	D	D	A	E	T	T	S	R	A	A	E	S
	Matsuura.vac	V	L	N	V	K	H	E	R	P	V	N	D	A	E	T	T	S	R	A	T	D	S
	TCRB19	V	L	N	A	K	R	E	R	P	V	N	D	A	E	T	T	S	R	A	A	E	S
	RA27/3	V	L	N	A	R	H	K	R	S	V	N	E	A	E	T	T	S	R	A	A	E	S

Fig. 4. Comparison of the amino acid residues among seven RuV wt strains and six vaccines. The amino acid sequences were compared among 13 RuV strains (seven wt strains and six vaccines), and residues with variations were noted. (A) NSPs. (B) SPs. Shaded symbols indicate amino acid residues in minority groups among the 13 strains. Numbers indicate the amino acid positions. Known or predicted functional domains [20,22,44,45] are indicated in the top rows. MT: methyltransferase domain; X: X domain; Pro: protease domain; Hel: helicase domain; RdRp: RNA-dependent RNA polymerase domain; C_{SP}: signal peptide of the capside protein; $E2_{TM}$: transmembrane domain of E2; $E1_{TM}$: transmembrane domain of E1.

B

		C																			
		11	18	22	26	34	48	60	64	67	69	71	72	76	87	95	141	175	226	254	260	283
Wt	M33	D	A	A	G	S	T	P	R	A	A	R	K	R	S	K	L	I	T	T	H	A
	Matsuba.GMK5	D	A	A	E	S	S	R	G	G	G	R	R	R	S	K	L	T	T	S	H	V
	Matsue.JPN68	A	A	A	E	S	S	R	G	G	G	R	R	R	S	K	L	T	T	S	H	A
	TO-336wt	D	A	A	E	S	S	R	G	G	G	L	R	R	S	K	L	T	T	S	H	A
	TO336.GMK5	D	A	A	E	S	S	R	G	G	G	L	R	R	S	K	L	T	T	S	H	A
	Matsuura.B3	D	A	A	E	S	S	R	G	G	G	R	R	R	S	K	L	T	T	S	H	A
	Therien	D	A	A	E	S	S	R	G	G	G	R	R	R	T	K	L	T	T	S	H	A
Vac	Matsuba.vac	G	A	A	E	P	S	R	G	G	G	R	K	R	S	K	L	T	T	S	H	A
	KRT	G	A	A	E	P	S	R	G	G	G	R	K	R	S	K	L	T	S	S	H	A
	TO-336.vac	D	A	A	E	S	S	R	G	G	G	L	R	R	S	K	L	T	T	S	H	A
	Matsuura.vac	D	A	V	E	S	S	R	G	G	G	R	R	K	S	K	P	T	T	S	Y	V
	TCRB19	D	A	A	E	S	S	R	G	G	G	R	R	R	S	E	L	T	T	S	H	A
	RA27/3	D	T	A	E	S	T	R	G	G	G	R	R	R	T	K	L	T	T	S	H	A

		C_{SP}	E2																$E2_{TM}$		E2	$E2_{TM}$
		292	306	307	313	314	319	351	404	405	411	412	413	422	446	485	491	505	534	535	539	558
Wt	M33	A	A	D	M	P	R	H	S	L	Y	I	A	P	Y	I	E	T	S	L	F	A
	Matsuba.GMK5	A	A	D	T	L	R	H	P	L	S	T	T	A	H	V	E	T	S	L	V	A
	Matsue.JPN68	A	A	D	T	L	R	H	P	F	S	T	T	A	H	V	E	T	S	L	L	A
	TO-336wt	A	A	D	T	L	R	H	P	F	S	T	T	A	H	V	E	T	S	L	L	A
	TO336.GMK5	A	A	D	T	L	R	H	P	F	S	T	T	A	H	V	E	T	S	L	L	A
	Matsuura.B3	A	A	D	T	L	R	H	P	F	S	T	T	A	H	V	E	T	S	L	L	A
	Therien	T	A	D	T	L	C	Y	P	L	S	T	T	A	H	V	E	A	S	L	L	A
Vac	Matsuba.vac	A	V	H	T	P	R	H	S	L	S	T	T	P	H	V	E	T	P	P	L	A
	KRT	A	V	H	T	P	R	H	S	L	S	T	T	P	H	V	E	T	P	P	L	A
	TO-336.vac	A	A	D	T	L	R	H	P	F	S	T	T	A	H	V	E	T	S	L	L	A
	Matsuura.vac	A	A	D	T	L	R	H	P	F	S	T	T	A	H	V	G	T	S	L	L	A
	TCRB19	A	A	D	T	L	R	H	P	L	S	T	T	A	H	V	E	T	S	L	L	A
	RA27/3	A	A	D	T	L	R	H	P	L	S	T	T	A	H	V	E	T	S	L	L	T

		E1																		$E1_{TM}$
		587	599	609	650	756	759	785	792	801	873	890	915	919	953	954	959	962	980	991	1041
Wt	M33	T	T	G	T	V	N	L	Y	G	I	H	A	A	T	V	V	F	Q	T	P
	Matsuba.GMK5	T	T	R	T	V	N	L	Y	G	I	H	A	A	T	V	V	F	Q	S	L
	Matsue.JPN68	T	T	R	T	V	N	L	Y	G	I	H	A	A	T	V	V	F	Q	S	L
	TO-336wt	T	T	R	T	A	N	L	Y	G	I	H	A	A	T	V	V	F	Q	S	L
	TO336.GMK5	T	T	R	T	V	N	L	Y	G	I	H	A	A	T	V	V	F	Q	S	L
	Matsuura.B3	T	T	R	T	V	N	L	Y	G	I	H	A	A	T	V	V	F	Q	S	L
	Therien	T	A	R	A	V	N	L	Y	G	I	H	A	T	T	V	L	V	Q	T	P
Vac	Matsuba.vac	A	T	R	T	V	D	M	Y	G	I	H	T	A	T	V	V	F	Q	S	L
	KRT	A	T	R	T	V	D	M	Y	G	I	H	T	A	T	V	V	F	R	S	L
	TO-336.vac	T	T	R	T	A	N	L	Y	G	I	R	A	A	T	L	V	F	Q	S	L
	Matsuura.vac	T	T	R	T	A	D	L	Y	S	I	H	A	A	T	V	V	F	Q	S	L
	TCRB19	T	A	R	T	V	N	L	Y	G	M	H	A	A	A	V	V	F	Q	S	L
	RA27/3	T	A	R	T	V	N	L	H	G	I	H	A	T	T	L	L	F	Q	S	L

Fig. 4. (Continued).

(Figs. 3 and 4). Except for the A1020T substitution in P150, Matsuura.B3 possessed the identical amino acid sequence to the consensus sequence among the other three wt strains, TO-336.GMK5, RVi/Matsue.JPN/68, and Matsuba.GMK3, in the same cluster (Figs. 2 and 4). These data suggest that Matsuura.vac acquired the 19 amino acid substitutions under the attenuation process (Fig. 3). Eight of these substitutions were in P150 (Figs. 3 and 4). Among these substitutions, P235S was in the methyltransferase (MT) domain [20,22], E907Q and R963C were in the X domain with unknown functions [20,21], and A1166V was in the protease domain [20–23] (Fig. 4A). A1166V was also located in the helical structure of the CaMBD (amino acid positions 1152–1183) in the protease domain [24]. Two substitutions (A1815T and E1921D) were found in P90, and both were located in the RNA-dependent RNA polymerase domain [20,21] (Fig. 4A). The C, E2, and E1 SPs had five, one, and three substitutions, respectively (Fig. 4B).

3.5. No common substitutions are found in vaccine strains, but some substitutions are shared by specific vaccine strains

Matsuba.vac and KRT shared many amino acid substitutions (Fig. 4). TCRB19 and RA27/3 also shared some amino acid substitutions (Fig. 4). However, despite these common features of the Japanese rubella vaccine strains, no consensus amino acid changes were found among them (Fig. 4). Regarding the molecular determinant for the ts phenotype, Sakata et al. [12] suggested that a Y1042H substitution in P150 is responsible for the ts phenotype of KRT. Matsuba.vac possessed the same substitution (Fig. 4A). Interestingly, TCRB19 also had a tyrosine-to-cysteine substitution at the same position (Fig. 4A). Therefore, KRT, Matuba.vac, and TCRB19 may exhibit the ts phenotype via the same molecular mechanism.

3.6. TO-336.vac has acquired wt phenotypes by second-site mutations in the protease domain of P150

A TO-336.vac-derived mutant clone, designated TO-336.rev, was generated by passages of TO-336.vac in RK13 cells at 39 °C. Unlike TO-336.vac, TO-336.rev was able to replicate in RK13 cells at 39 °C, and its virus titer at 5 days p.i. was as high as that of TO-336.GMK5 (Fig. 5). The entire genome sequence of TO-336.rev was determined, and compared with that of TO-336.vac. A total of nine nucleotide substitutions were found in the genome of TO-336.rev (Table 1). Two of these substitutions were non-synonymous, and both were located in the protease domain of P150 (Table 1). These mutations caused asparagine-to-threonine and alanine-to-valine substitutions at amino acid positions 1126 and 1277 (N1126T

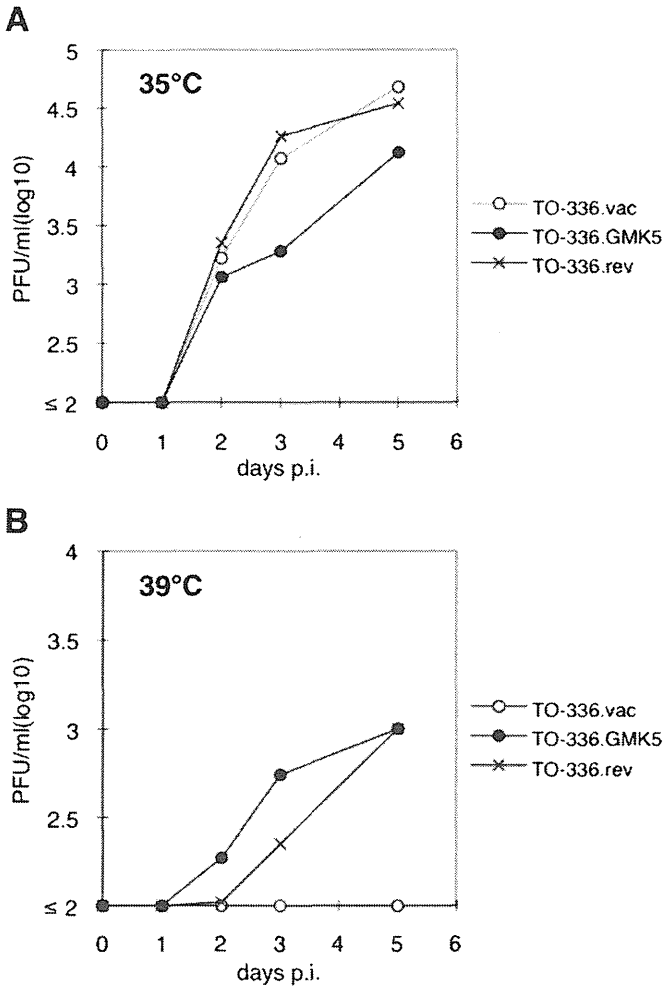

Fig. 5. Growth kinetics of TO-336.rev at 35 °C and 39 °C. RK-13 cells were infected with RuV strains at a MOI of 0.01 and incubated at 35 °C (A) or 39 °C (B). The infectious titers of the culture supernatants were determined by plaque assays. Closed and open circles indicate TO-336.GMK5 and TO-336.vac, respectively. Saltires indicate TO-336.rev.

and A1277V), respectively (Table 1). TO-336.vac possessed three amino acid substitutions in the NSPs compared with TO-336.GMK5 (Figs. 3 and 4A). Therefore, N1126T and A1277V were not direct reversions to the residues of TO-336.GMK5, but instead were second-site mutations that rendered TO-336.vac able to grow at 39 °C. These data brought the protease domain of the P150 protein to our attention.

3.7. Reduced stability of an NSP-derived peptide at 39 °C is correlated with reduced virus growth at that temperature (ts phenotype)

Chen et al. [16] analyzed the protease activities of RuV NSPs using NSP-derived peptides of varying lengths. We used one of these NSP-derived peptides corresponding to amino acid positions 994–1548 possessing FLAG tags at the amino-terminus ($NSP_{994–1548}$). Since the peptide retains the ability to cleave itself behind the amino acid position 1301 [16], the anti-FLAG antibody was expected to detect both uncleaved and cleaved forms of the peptide. The $NSP_{994–1548}$ peptide of TO-336.vac (TO-336.vac-$NSP_{994–1548}$) and that containing the residues of TO-336.GMK5 at positions 1159 and 1351 (TO-336.vac-$NSP_{994–1548}$(S1159N/D1351N)) were expressed in cells at 35 °C or 39 °C (Fig. 6A, TO-336.vac and S1159N/D1351N). A TO-336.vac-$NSP_{994–1548}$ mutant (C1152S), which lacks the protease activity, was expressed as a control (Fig. 6A, C1152S). Both the TO-336.vac-$NSP_{994–1548}$ and TO-336.vac-$NSP_{994–1548}$(S1159N/D1351N) were cleaved efficiently, and much stronger signals were detected for cleaved forms, when compared to the signals for uncleaved forms, at both temperatures (Fig. 6A). These data showed that the protease activity of TO-336.vac is not significantly affected by the mutations at positions 1159 and 1351. However, it was noted that the expression level of TO-336.vac-$NSP_{994–1548}$ became lower than those of TO-336.vac-$NSP_{994–1548}$(S1159N/D1351N) at 39 °C (Fig. 6A). It was more evident, when expression levels were analyzed at 3 days posttransfection (Fig. 6B) than at 1 day posttransfection (Fig. 6A). TO-336.vac-$NSP_{994–1548}$ peptides with the residues of TO-336.rev at positions 1126 and/or 1277 also showed similar protease activities (Fig. 6C). These peptides with various mutations were expressed in cells at 35 °C, and subsequently cultured

Table 1
Nucleotide and amino acid differences between TO-336.vac and the related viruses.

Region	Nucleotide				Amino acid			
	Position	TO-336.GMK5	TO-336.vac	TO-336.rev	Position	TO-336.GMK5	TO-336.vac	TO-336.rev
5′ UTR	36	U	C	C	N/A			
P	448	U	C	C	136	–	–	–
150	1327	U	C	C	429	–	–	–
	1708	U	C	C	556	–	–	–
	1757	C	U	U	573	His	Tyr	Tyr
	3417	A	A	C	1126	Asn	Asn	Thr
	3516	A	G	G	1159	Asn	Ser	Ser
	3781	C	C	U	1247	–	–	–
	3793	C	C	A	1251	–	–	–
	3870	C	C	U	1277	Ala	Ala	Val
	3946	U	U	C	1302	–	–	–
P90	4091	A	G	G	1351	Asn	Asp	Asp
J-UTR	6463	C	C	A	N/A			
C	6583	C	U	U	24	–	–	–
	6649	C	U	U	46	–	–	–
	6958	C	U	U	149	–	–	–
E1	8778	U	C	C	756	Val	Ala	Ala
	9013	U	U	C	834	–	–	–
	9180	A	G	G	890	His	Arg	Arg
	9371	G	C	C	954	Val	Leu	Leu
3′	9712	U	U	C	N/A			
UTR	9742	C	C	U	N/A			

N/A: not applicable, –: silent mutation.

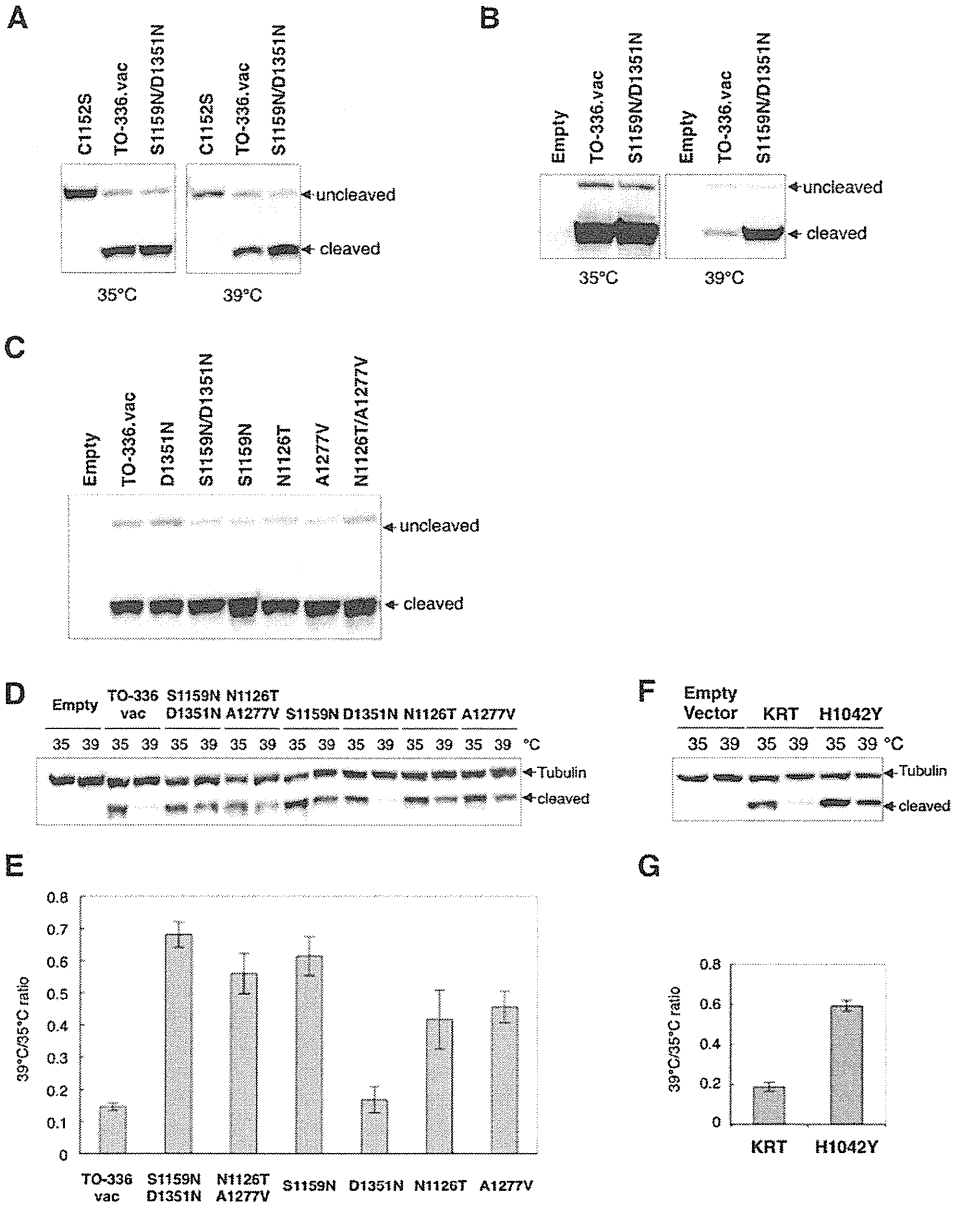

Fig. 6. Analysis of the thermal stabilities of NSP-derived peptides. (A and B) Using expression plasmids, an $NSP_{994-1548}$ peptide of TO-336.vac (TO-336.vac-$NSP_{994-1548}$) and that possessing the amino acid substitutions S1159N and D1351N (TO-336.vac-$NSP_{994-1548}$(S1159N/D1351N)) were expressed in cells at 35 °C or 39 °C. TO-336.vac-$NSP_{994-1548}$ possessing a C1152S mutation was also expressed as a control to show an uncleaved form of the peptide. Expression levels were analyzed at 1 day (A) and 3 days (B) after transfection of the plasmids. Empty; an expression plasmid lacking an $NSP_{994-1548}$ insert. (C) TO-336.vac-$NSP_{994-1548}$ peptides possessing the amino acid substitutions S1159N, D1351N, D1126T, and A1277 V individually or in combination were expressed in cells at 35 °C, and expression levels were analyzed at 1 day after transfection of the plasmids. Empty; an expression plasmid lacking an $NSP_{994-1548}$ insert. (D) An $NSP_{994-1548}$ peptide of TO-336.vac (TO-336.vac-$NSP_{994-1548}$) and those possessing the amino acid substitutions S1159N, D1351N, D1126T, and A1277 V individually or in combination was expressed in cells at 35 °C using expression plasmids. After 1 day of culture with the expression plasmids at 35 °C, the cells were cultured with cycloheximide to inhibit *de novo* protein synthesis for 2 days at 35 °C or 39 °C. Tubulin was detected as an internal control. Empty; an expression plasmid lacking an $NSP_{994-1548}$ insert. (E) Quantification of the data shown in (D). The ratios of the expression levels of the NSP peptides(cleaved form) at 39 °C and 35 °C are shown. The data represent the means ± standard errors of triplicate experiments. (F) $NSP_{994-1548}$ of KRT (KRT-$NSP_{994-1548}$) and that possessing an H1042Y substitution (KRT-$NSP_{994-1548}$(H1024Y)) were subjected to the same experiments described for (D). (G) Quantification of the data shown in (F). The data represent the means ± standard errors of triplicate experiments.

with cycloheximide to inhibit *de novo* synthesis of the peptides for 2 days at 35 °C or 39 °C (Fig. 6D). Fig. 6E shows the ratios of expression levels of the peptide ($NSP_{994-1301}$) at 39 °C and 35 °C (39 °C/35 °C ratios). Only cleaved forms, $NSP_{994-11301}$, were shown, since uncleaved forms were barely detectable. These data showed that TO-336.vac-$NSP_{994-1301}$ was unstable at 39 °C (Figs. 6D and E, TO-336.vac), whereas TO-336.vac-$NSP_{994-1301}$(S1159N/D1351N) was stable (Figs. 6D and 7E, S1159N/D1351N). A peptide containing the residues of TO-336.rev at positions 1126 and 1277 (TO-336.vac-$NSP_{994-1301}$(N1126T/A1277V)) also exhibited high stability at 39 °C (Figs. 6D and E, N1126T/A1277V). The effects of individual mutations at positions 1159, 1351, 1126, and 1277 were analyzed. The data revealed that the peptide possessing S1159N was as stable as TO-336.vac-$NSP_{994-1301}$(S1159N/D1351N) (Figs. 6D and E, S1159N). The D1351N substitution had no effect on the stability of $NSP_{994-1301}$ at 39 °C (Figs. 6D and E, D1351N). These data suggest that the N1159S mutation causes the ts phenotype of TO-336.vac, and that N1351D only exerts a neutral effect. On the other hand, both types of peptides with N1126T or A1277V showed moderate stability at 39 °C (Figs. 6D and E, N1126T and A1277V). These data